Meteoritics & Planetary Science 40, Nr 6, 895–916 (2005)
Abstract available online at http://meteoritics.org

Genesis—An artificial, low velocity "meteor" fall and recovery: September 8, 2004

D. O. REVELLE[1*], W. EDWARDS[2], and T. D. SANDOVAL[1, 3]

[1]Atmospheric, Climate, and Environmental Dynamics, Earth and Environmental Sciences Division, Los Alamos National Laboratory, Los Alamos, New Mexico 87545, USA
[2]Department of Earth Sciences, University of Western Ontario, London, Ontario, N6A 5B7, Canada
[3]Present address: DX-2, Material Dynamics Group, Los Alamos National Laboratory, Los Alamos, USA
[*]Corresponding author. E-mail: revelle@lanl.gov

(Received 28 January 2005; revision accepted 26 April 2005)

Abstract–On September 8, 2004, Genesis, a manmade space capsule, plummeted to Earth after almost three years in space. A ground-based infrasound array was deployed to Wendover, Nevada, to measure the "hypersonic boom" from the reentry, since the expected initial reentry speed of the body was about 11 km/sec. Due to the complete failure of its dual parachute system, we had a unique opportunity to assess the degree of reliability of our previously developed relations for natural meteors and bolides to analyze this well-characterized manmade body. At ~20–50 km from the nominal trajectory, we succeeded in recording over two minutes of infrasonic signals from Genesis.

Here we report on subsequent analyses of these infrasonic data, including an assessment of the expected entry characteristics on the basis of a bolide/meteor/fireball entry model specifically adapted to modeling reentering manmade objects. From these simulations, we were able to evaluate the line source blast wave relaxation radius, the differential acoustic efficiency, etc., to compute an approximate total power balance during entry. Next, we analyzed the detailed signals arriving from Genesis using a numerical, signal detection and wave processing software package (Matseis/Infra_Tool). We established the initial and subsequent arrivals and evaluated its plane wave back azimuths and elevation arrival angles and the degree of maximum, pair-wise cross-correlation, its power spectrum, spectrogram analysis, standard seismic f-k analysis, etc. From the associated entry parameters, we computed the kinetic energy density conservation properties for the propagating line source blast waves and compared these predictions against observed ground-based infrasound amplitude and wave period data as a function of range. We discovered that previously computed differential acoustic efficiencies were unreliable at Mach numbers below about 10. This is because we had assumed that a line source explosion was applicable, whereas at very low Mach numbers, typical of recovered meteorites, the detailed source characteristics are closer to those of supersonic objects. When corrections for these unphysical, very high efficiencies were made, agreement between theory and observations improved. We also made an assessment for the energy of the blast wave source from the ground-based infrasound data using several other techniques that were also adapted from previous bolide studies. Finally, we made a top-down–bottom-up assessment of the line source wave normals propagating via refraction downward into the complex middle atmospheric environment. This assessment proved to be generally consistent with the digital signal processing analysis and with the observed time delay between the known Genesis reentry and the infrasonic observations.

INTRODUCTION AND OVERVIEW

Large Meteoroid Entry

Upon entry to Earth's atmosphere, large meteoroids have initial velocities ranging from 11–73 km/sec and can produce strong shock waves while ablating, fragmenting, decelerating, and producing copious amounts of luminosity with heat transfer flow regimes ranging from the extremes from free-molecular to continuum. In this process, we must deal with their generally unknown characteristics of shape, radius, speed, composition, degree of porosity, and rotation and tumbling. We had previously developed detailed algorithms for evaluating their expected entry characteristics as well as the concomitant production of light, heat, mechanical waves (including acoustic-gravity waves), ionization, and so forth.

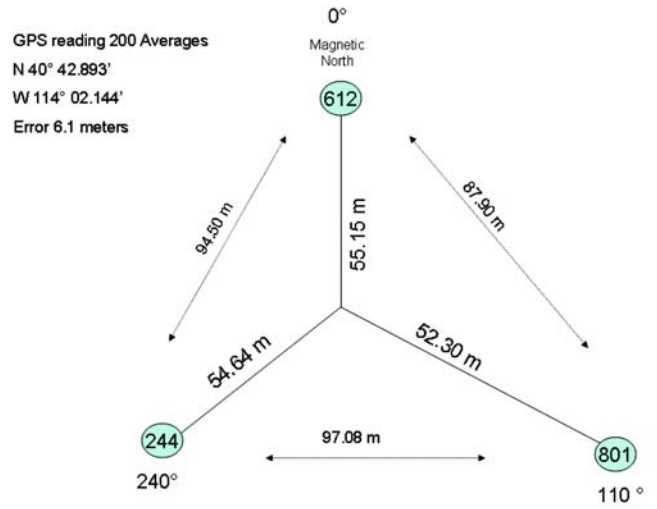

Fig. 1a. Wendover infrasound array details.

Since the Genesis capsule's dual parachutes did not deploy at all during entry, we felt that we had a very good surrogate for an artificial, albeit low-speed, meteor entry that could be extensively studied and compared against our "standard" repertoire of bolide evaluation techniques. Although we systematically planned for the ground-based infrasound measurements (discussed in detail below), we did not plan to write this paper. It occurred simply because the data begged to be systematically analyzed.

The Genesis Experiment

We monitored the reentry at the local airport in Wendover, Nevada, at 40.7154° latitude, –114.0357° longitude. The Earth and Environmental Sciences Division of the Los Alamos National Laboratory, with additional financial support from Dr. Peter Jenniskens of the NASA Ames Research Center and from the International, Space and Response (ISR) Division of the Research and Development Program Office and its leader Dr. John Szymanski, decided to deploy a temporary three-element infrasound array (Fig. 1a) with the closest possible horizontal range to the Genesis ground track of 26.1 km, corresponding to a source altitude of 43.07 km. This was a NASA pre-entry "nominal" trajectory; for further details, see Fig. 1b, which has a geographic depiction of the NASA flight track and its location with respect to the Wendover temporary infrasound array and to the seismic stations searched (this information was based on preflight expectations, but this altitude is still well above the 30 km height where the first main parachutes were to be deployed, so the corresponding values should still be totally acceptable). Table 1, in addition to listing some of the most important physical properties of the Genesis spacecraft, also lists in some detail the properties of forthcoming NASA and the Japanese Aerospace Exploration Agency (JAXA) experiments (Stardust and Hayabusa, respectively).

Briefly, a manmade space capsule, which had been in space for nearly three years, with a mass of 225 kg reentered the atmosphere after separation from the main spacecraft and subsequently plunged into the atmosphere at 11 km/sec at an initial entry angle of about 8 degrees. NASA had done a complete reentry analysis of this body with a charring ablation heat shield for protection of the spacecraft instruments (R. Wiens, personal communication 2004). This is the first time that this type of heat shield had been used since the Mercury-Gemini-Apollo era. The Genesis experiment was carrying a very valuable cargo of solar wind particle track detections (R. Wiens, personal communication 2004). Its unfortunate ground impact (just as if it were a low-velocity meteorite entry) was our very good fortune from a meteor entry point of view.

PREDICTION OF THE GENESIS ENTRY ENVIRONMENT

It was challenging to model a real reentry where many parameters are known, unlike the usual bolide entry cases that we have done repeatedly in the past. Our standard bolide model (ReVelle et al. 2004; ReVelle Forthcoming) incorporates a number of useful features and physics necessities, including laminar versus turbulent convective heat transfer through the gas cap, and full shock wave radiative heating calculated independently of the gas cap opacity (not strictly in the "diffusion" approximation). It also includes a triggered progressive fragmentation model (TPFM) that results in a cascade of continuous fragmentation once it is initiated by the stagnation pressure exceeding the body's breaking strength. The latter values are also explicitly included within the scheme for all known meteoroid types, but this breakup feature was intentionally turned off during our modeling efforts below. All heating and momentum functions were physically linked as a function of the various flow regimes encountered during entry as mentioned earlier. The model can be run in either a homogeneous or a porous meteoroid mode and is capable of providing the expected luminous output (watts/steradian) in a panchromatic passband as well as a total power budget as a function of height or of time.

First, the theoretical modeling option that we had chosen to use in order to understand the Genesis entry assumes a homogeneous body that is certainly not applicable to this complex capsule. Second, we have a porous body option in the entry code, but this is also clearly not a case of uniform porosity, as was assumed in our code development. What is most important for the case of ballistic, non-lifting entry at low-entry velocities is, first, the mass to area ratio (proportional to the modified ballistic entry parameter), and second, the body radius and its associated shape and/or its changes during entry. Since Genesis is nearly spherical and we cannot rule out tumbling (this effect can be readily observed in the official NASA filming of the entry, that is, in

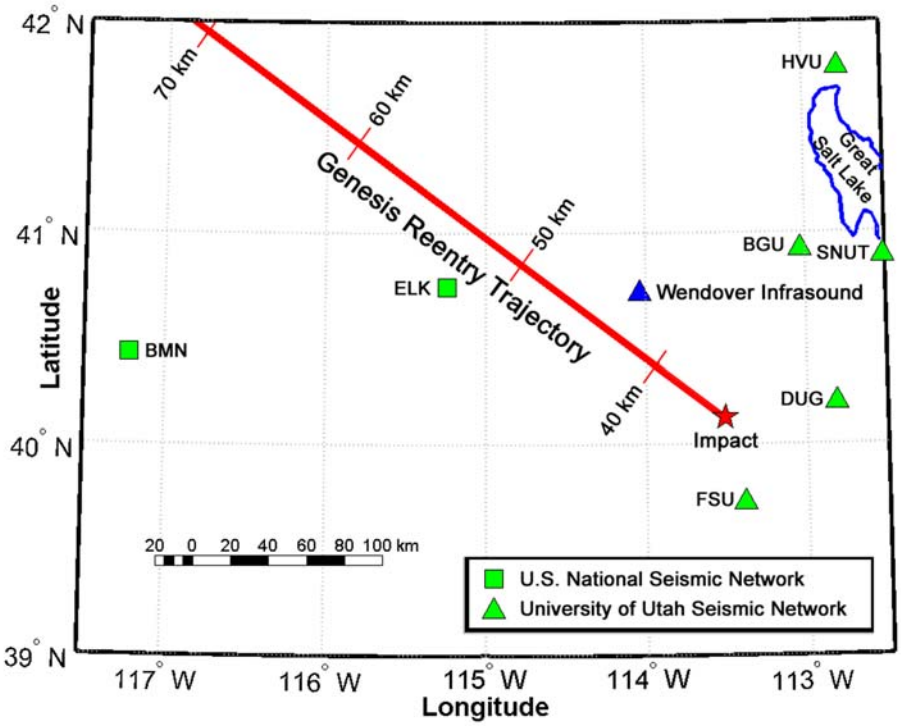

Fig. 1b. Geographical overview of Genesis entry.

Table 1. Genesis in comparison to other forthcoming entry vehicles.

	Genesis	Stardust	Hayabusa
Date	08 September 2004	15 January 2006	June 2007
Time (local)	9:54 a.m. MDT	3:00 a.m. MDT	3:00 a.m.
Mass (kg) *m*	225	45.8	18
Diameter *d*	1.52	0.811	0.40
Entry speed at 135 km (in km/sec)	11.0	12.9	12.2
Entry angle (degrees) θ	8.0	8.2	12.0
Spin rate (rpm)	15	15	2
Aerodynamic stability	not stable	not stable	stable
Peak heat rate (w/cm^2)	750	1200	~1500
Peak deceleration (Earth 'g's)	28	34	45
Peak brightness (from 100 km)	–	–	–
Landing site	UTTR, Utah	UTTR, Utah	Australia
Heat shield material	carbon-carbon	phenol-impregnated carbon ablator (PICA)	carbon phenolic ablator
Thickness	1.5" over insulator	2"	–
Sample returned	solar wind	comet dust, ISD	asteroid debris

addition to the nominal 15 revolutions/min imposed spin rate), we will assume for simplicity that a sphere adequately captures the shape of the body. We know the total capsule mass, so we can calculate the equivalent radius of a homogeneous sphere of uniform bulk density corresponding to, say, that of ceramic interior materials, i.e., ~1000–3000 kg/m^3. We used a typical value that was especially convenient, namely that of group II bolides, ρ_m = 2100 kg/m^3 (ReVelle 2002).

The bulk density that was finally chosen for the Genesis reentry spacecraft has not yet been calibrated in an absolute sense, but should be typical of the expected values, based on ceramic materials and on the uniform bulk density assumption necessary for the current meteor/bolide theory. Thus, it is necessary at this point to provide some degree of the expected altitude uncertainty and of the degree of successful calibration associated with this choice of the uniform material bulk density. First, for Genesis, with the low-entry velocity and the control provided by the ablative heat shield, a large degree of overall ablation is not expected during entry, even using our standard meteor/bolide theory. This means that for our ballistic entry model, uncertainties in

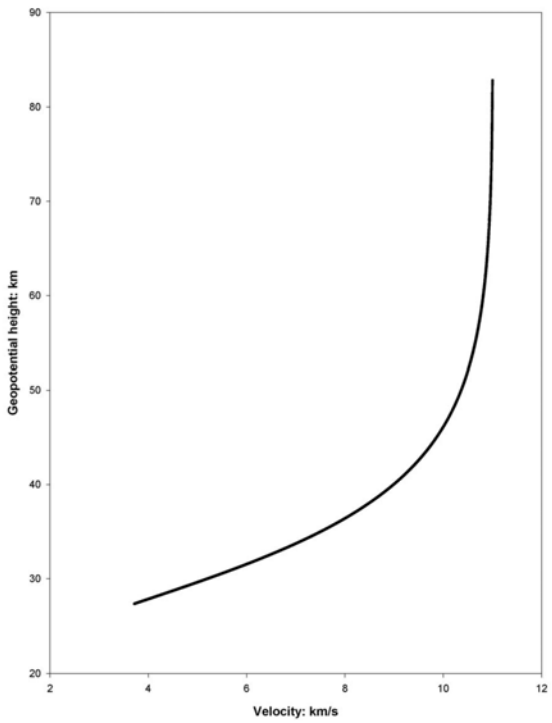

Fig. 2a. Entry environment predictions: velocity.

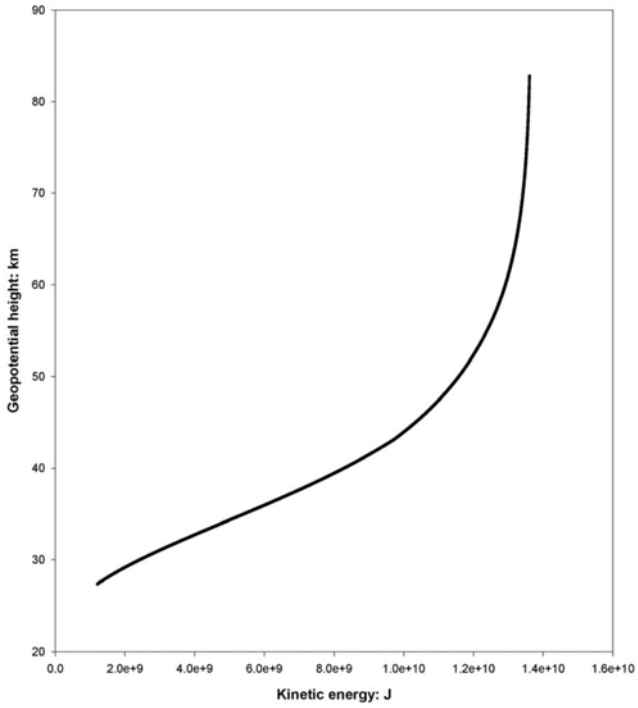

Fig. 2b. Entry environment predictions: kinetic energy.

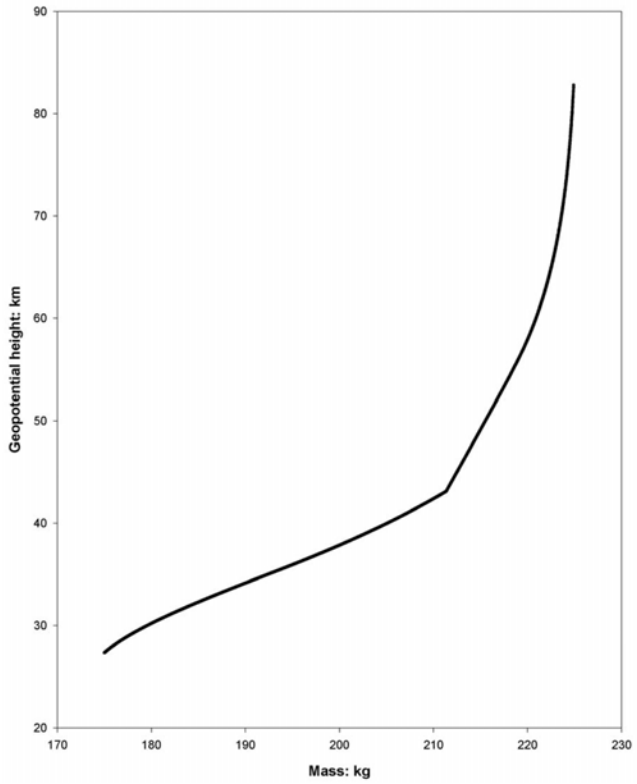

Fig. 2c. Entry environment predictions: mass loss.

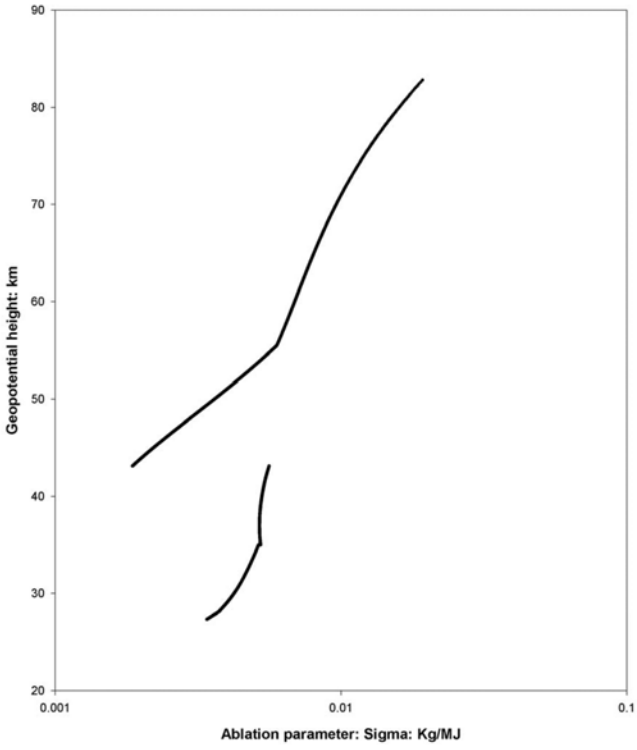

Fig. 2d. Entry environment predictions: ablation parameter, σ.

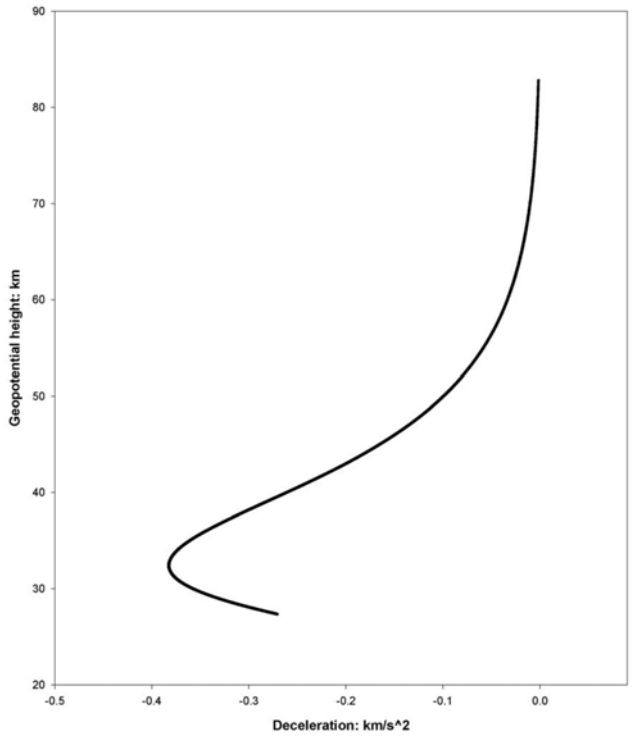

Fig. 2e. Entry environment predictions: deceleration.

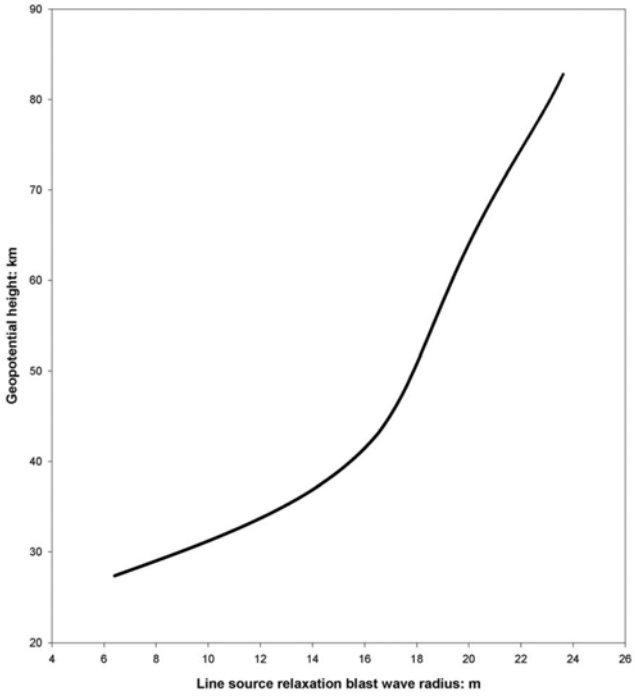

Fig. 2f. Entry environment predictions: line source blast radius.

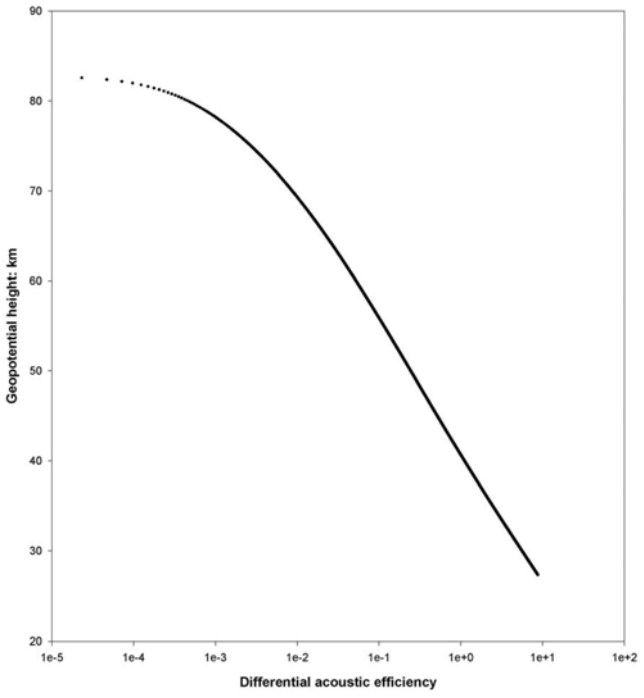

Fig. 2g. Entry environment predictions: differential acoustic efficiency.

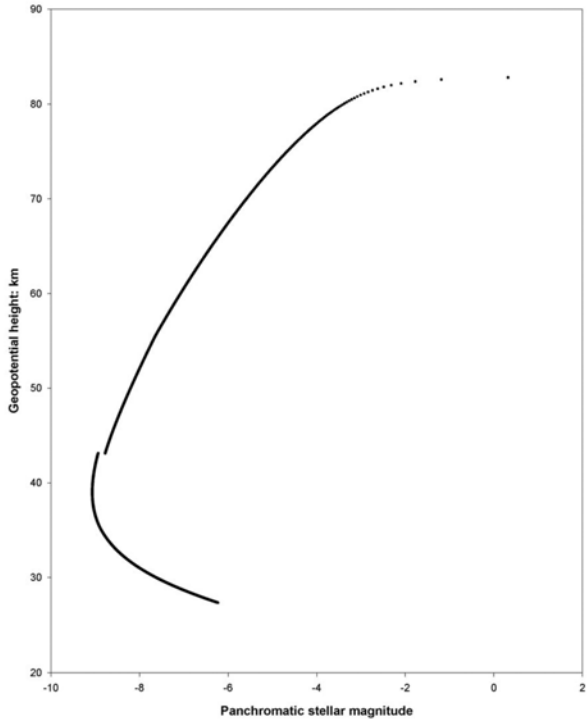

Fig. 2h. Entry environment predictions: panchromatic luminosity (at 100 km in the zenith).

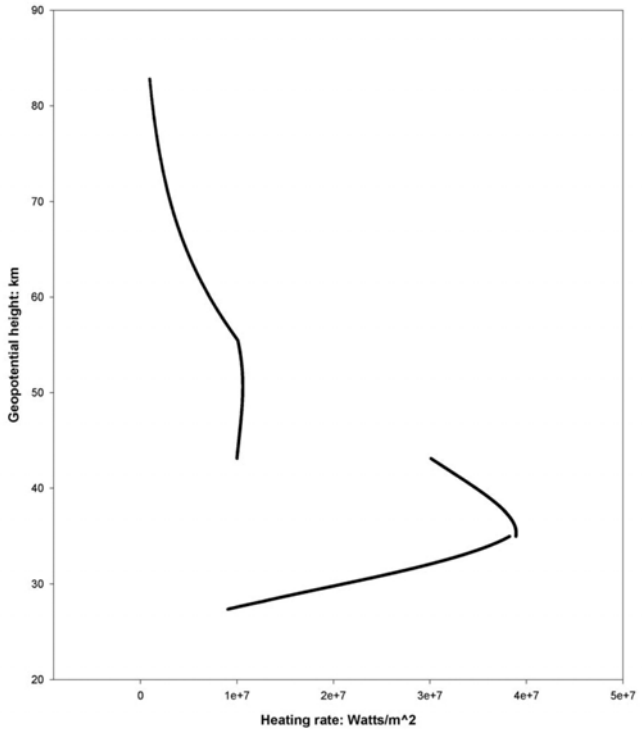

Fig. 2i. Entry environmental predictions: total heating rate.

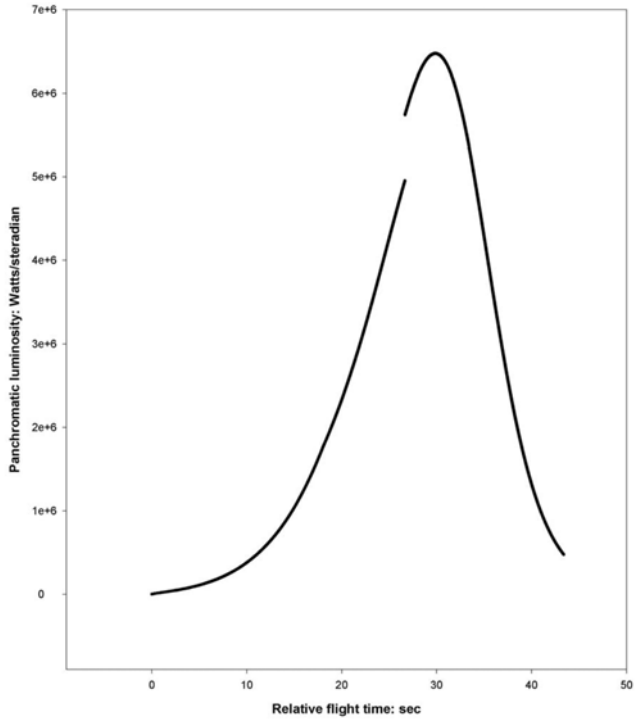

Fig. 2j. Entry environmental predictions: the power time curve.

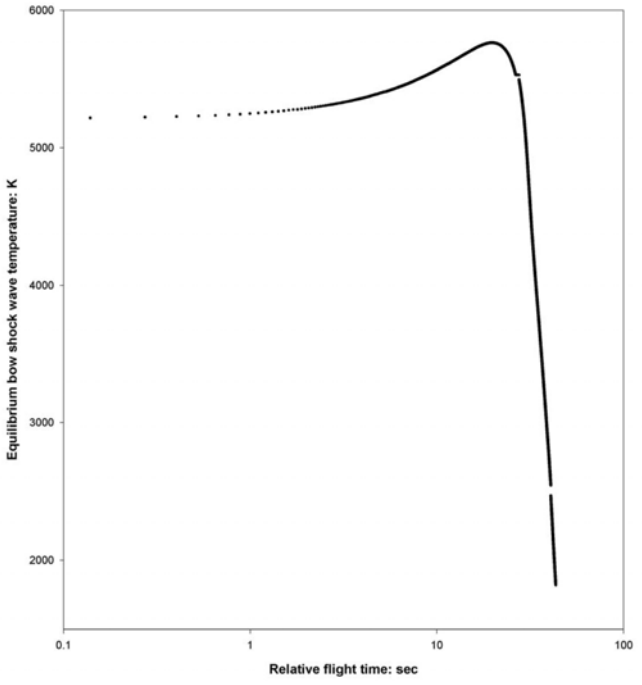

Fig. 2k. Entry environmental predictions: the equilibrium bow shock wave temperature.

the altitude of penetration are almost completely dominated by the modified ballistic entry parameter (ReVelle 1979), which is proportional to the mass to area ratio for the body (which is further proportional to the product of the radius times the bulk density for a specified shape factor). For a bulk density variation that is either a factor of two larger or smaller than the nominal assigned value, i.e., from $1.05 \cdot 10^3$ kg/m^3 to $4.2 \cdot 10^3$ kg/m^3 (with respect to $2.1 \cdot 10^3$ kg/m^3), altitude penetration differences of up to ±4–5 km (with upward altitude increases predicted for lower bulk densities and vice versa) are expected in an isothermal, hydrostatic model atmosphere with a pressure scale height of ~7 km. The predicted altitude of peak heating for the nominal bulk density was ~37 km (Fig. 2i). A separate entry dynamics solution, not presented here in detail, in which the turbulent boundary layer flow transition algorithm was intentionally turned off at all levels, predicted a peak heating altitude at ~56 km, for example, for the nominally assigned bulk density value. However, because of the relatively low heating prediction overall, this altitude difference in these nominal predicted heating peaks did not make a significant difference in the predicted end height (where luminosity ceases) for Genesis (with the turbulence-free solution ending ~1.5 km higher in altitude with a velocity of 4 km/sec at ~29 km for the turbulence-free boundary layer and ~27.5 km for the solution at a velocity of 4 km/sec with the turbulent boundary layer transition prediction allowed). Thus, with the stated bulk density uncertainty, the altitude of peak heating could actually be at a height of 35 ± 4–5 km (or for solutions without a turbulent boundary layer transition allowed, the predicted peak heating could occur at a height of ~56 ± 4–5 km). The official NASA peak heating altitude (without a turbulent boundary layer transition predicted) is ~60 km (R. Wiens,

Table 2. Inputs for entry dynamical and panchromatic luminosity calculations and wave normal path evaluations.

Initial radius (m)	0.2946
Initial velocity (km/sec)	11.0
Zenith angle of radiant (degrees)	82.0
Vector heading azimuth (degrees)	305.0
Shape factor (sphere)	1.209
Shape change factor (μ)	2/3 (no shape change allowed)
Kinetic energy depletion factor, *D* (99% KE depletion)	4.605
Homogeneous or porous model	Homogeneous
Uniform bulk density of the Genesis capsule	$2.1 \cdot 10^3$ kg/m^3
Ablation parameter, σ changes	Variable σ(z)
Atmosphere model type	Nonisothermal, hydrostatic atmosphere
Season of the year	Summer atmospheric model

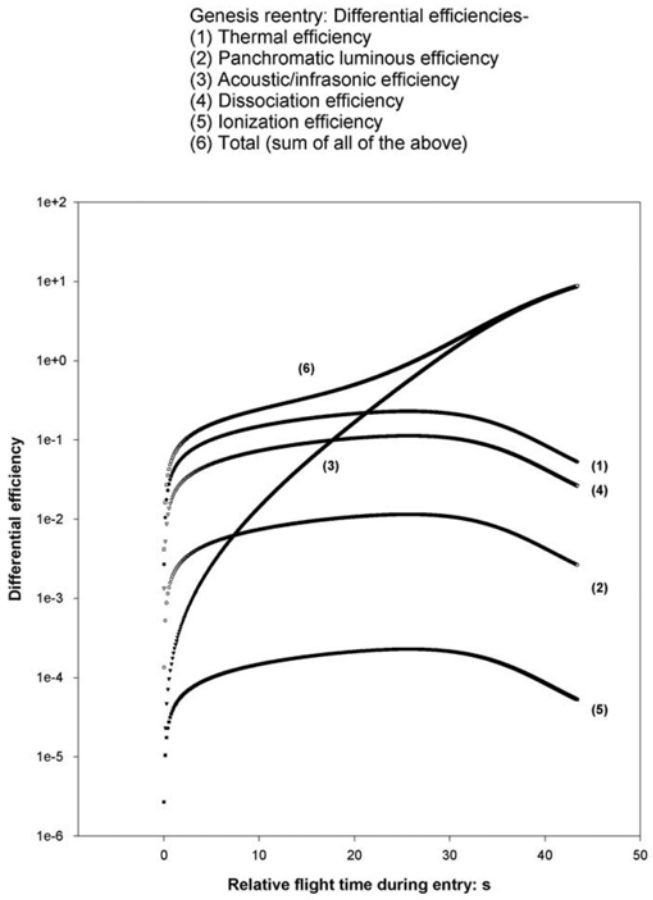

Fig. 3. Hypersonic aerodynamic total power balance and differential efficiencies: uncorrected for supersonic flow effects at low heights.

personal communication 2004). Thus, from these various comparisons, we can deduce that the actual nominal bulk density for Genesis is closer to ~$1.5 \cdot 10^3$ kg/m^3. Thus our proposed entry solutions are quite close to reality, given the uncertainties between various atmospheric models, drag coefficients for complex shapes, and so forth.

To match the corresponding mass value for a homogeneous sphere, the computed nominal radius is ~0.2946 m (compared to 0.76 m for the basic physical dimensions of the body, given in Fig. 2). Our initial theoretical calculations matched the mass to area of the body, since both are known precisely, but because it is not homogeneous throughout its interior, that approach was not acceptable. In the latter case, the formal computed mass/area ratio is ≅124.0 kg/m^2, which can be compared to the value we utilized for our final Genesis entry simulations, namely, 824.88 kg/m^2 (for a spherical shape). The latter value would imply a bulk density some 6.65 times lower than what we used, which may be physical for the capsule, but certainly does not apply to the homogeneous meteor model that we have used to simulate the Genesis entry. It should also be pointed out that we use a generalized ablation model for the entire object and not just the heat shield solution for a charring ablator typical of the Apollo and earlier reentry programs and, of course, available for the protection of the Genesis capsule during its entry.

Our entry inputs also correspond to a case of constant entry angle, θ as well which is also clearly not the case according to the preflight data (R. Wiens, personal communication 2004). We proceeded, however, with a constant entry angle solution (equal to the initial value at the interface entry altitude, where the body force component/mass along the trajectory just balances the acceleration due to gravity. This occurs at approximately 82.8 km.), since it is not expected for this angle to significantly change until much lower altitudes (approximately 35 km if the drogue shoots had deployed, and this actually occurred below approximately 10 km after terminal velocity had been reached for the reentry package without any chutes opened). This was reasonable, since the parachutes did not deploy at all as expected during entry.

With these values supplied to the entry code, we can proceed as described above. We have adapted an entry model (ReVelle 2001; ReVelle 2002) originally developed for modeling the ballistic entry of meteor-fireballs (bolides). Table 2 lists the inputs we have used to model the Genesis reentry, with some of the details taken from R. Wiens (personal communication 2004).

Below about 30 km for the NASA nominal planned reentry, the entry angle would become quickly nearly vertical, so that $Z_R = 0$ deg, due to the effects of the acceleration due to gravity in the absence of significant horizontal winds.

Velocity, Kinetic Energy, Mass Loss, and the Ablation Parameter

In Figs. 2a–2d, we have plotted the following predicted parameters for the Genesis entry versus either height or time, respectively: velocity, kinetic energy, mass loss (overall 22% was predicted, if this were a real bolide) and the expected corresponding ablation parameter, σ. As expected, all

parameters are quite reasonable in magnitude, given the rather low entry velocity. The only exception was the ablation parameter, which jumped suddenly around 43 km due to the prediction of a laminar to turbulent, gas-cap boundary layer transition. Computer calculations that were done with the turbulent boundary layer (gas-cap) transition removed agreed much better with the official NASA predictions for the Genesis reentry behavior (R. Wiens, personal communication 2004).

Deceleration, Line Source Blast Wave Radius, and the Differential Acoustic Efficiency

In Figs. 2e–2g, we have plotted the deceleration, the line source blast wave relaxation radius, and the differential acoustic efficiency parameters. Reasonable agreement in both geopotential height and in terms of the number of g's experienced during entry was once again found between our deceleration predictions and those made by NASA in advance (R. Wiens, personal communication 2004). Blast wave radii for an assumed non-breaking body were found in the range from ~10–30 m, depending explicitly on height. We have used the line source explosion blast radius formulation <M · d throughout as utilized in our bolide computations. The lack of complete applicability of this spatial scale to the very low speed supersonic flow regime is discussed briefly later. This scale also has consequences for the very large differential acoustic efficiency determined at low heights, as will also be discussed.

Panchromatic Luminosity, the Power-Time Curve, the Total Heating Rate, and the Equilibrium Bow-Shock Wave Air Temperature

In Figs. 2h–2k, we have plotted the panchromatic luminosity (expressed in stellar magnitude as observed at 100 km altitude in the zenith), the total heating rate (expressed in watts/m^2), the power-time curve (expressed in watts/steradian) and the equilibrium, chemically reacting flow, bow shock wave air temperatures (in °K) averaged across the frontal cross sectional area using a local oblique shock wave flow angle equalling 30°. (Using a local normal shock wave flow angle equalling 90°, the stagnation point computed air temperatures are all a factor of two greater at all of the computed heights). These values have been computed using a standard, albeit iterative, hypersonic aerodynamic approach using very detailed curve fits of the thermodynamic properties of very high enthalpy air (Anderson 2000). Our computed total heating rate is much larger than that officially predicted by NASA, since a gas-cap turbulent boundary layer transition from laminar to turbulent was predicted during the entry, as noted earlier for the ablation parameter presented in Fig. 2d. Peak shock wave temperatures in this case briefly exceeded 5700 °K (or >~11,400 °K for a normal shock front at the stagnation point).

An optical video recording of the Genesis entry was also made in Nevada by A. Hildebrand and M. Beech (Department of Physics, University of Calgary). Problems with decoding this video have prevented us from using it in this paper at this time. Numerous problems still exist with trying to extract this data, however (P. Brown, personal communication 2004).

Total Power Budget

Following ReVelle et al. (2004), we have also plotted all of the various differential efficiencies predicted for the Genesis entry (Fig. 3). The only unusual value is the differential acoustic efficiency below ~35 km which exceeds unity (100%). As a direct result, of course, the corresponding total power budget exceeds 100% below this altitude as well. Later on, we will show that this is due physically to the fact that we had used the hypersonic line source blast wave analog theory throughout to make pressure wave amplitude predictions. Below Mach numbers in the range of 10–20, we need to construct a transitional approach to a fully supersonic flow theory result, which we have shown later will predict significantly smaller differential acoustic efficiency values, as well as signal amplitudes and shorter duration pulses at close range. In all other ways, our results show that we have accounted for a very large percentage of all of the power lost during atmospheric entry for Genesis. The only exception to this statement is at the very earliest time of entry, when presumably more thermal power in the form of heat was generated than we have presently predicted.

MEASUREMENTS DURING ENTRY

Deployment of the Infrasound Array: Wendover, Nevada

All of our detection equipment was driven by government van from Los Alamos, New Mexico, to Wendover, Nevada, with just enough time to set up the array and check out the equipment for about 24 hours prior to the reentry event. The pieces of primary field equipment deployed were:

- Three Chaparral low-frequency capacitance differential microphones: Response: 3 dB down nominally at 0.02 and 300 Hz
- Teledyne-Geotech 24 bit digitizer and the GPS timing unit
- Six sets of 16-m long, porous soaker hoses at equal angular spacing at each microphone (wind-noise reduction filters)

The digital sampling rate employed was 50 Hz, so that we have an imposed sampling cut-off frequencies in all of our FFT (Fast Fourier Transform) calculations corresponding to frequencies below the concomitant Nyquist value, i.e., 25 Hz. The deployment arrangement at the Wendover, Nevada, airport is indicated in Fig. 1a. The location of the array was some 25–40 km to the northeast of the expected entry flight path. At the expected time of the reentry, the LANL

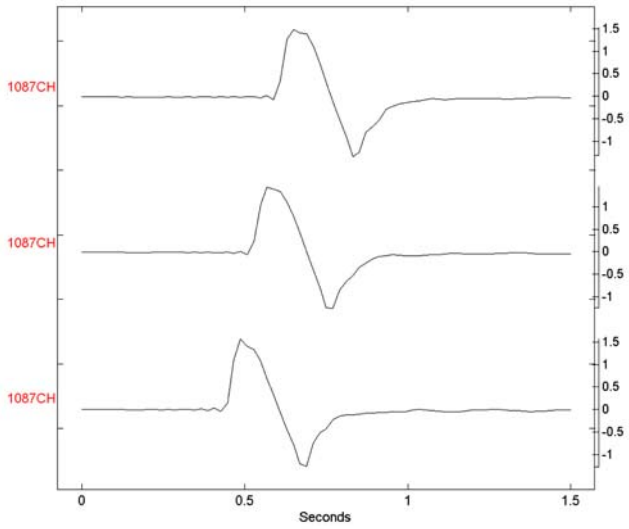

Fig. 4. Initial N wave arrivals (filtered).

infrasound team was located on a high observation tower at the airport. Two of the three people present heard two distinct booms from the event, but in the excitement of the moment, the second boom could easily have been missed by the third person. The event was not witnessed visually at our location at all, probably due to the lack of contrast caused by the relatively high local position of the sun in the sky by about 10 a.m. It was also near the time of the autumnal equinox.

Recordings of the infrasound from the Genesis reentry were obtained with a ground-based acoustic array similar to the single microphone measurements made on each ship, which were placed directly beneath the planned ground track during the Apollo reentries of the 1970s (Hilton et al. 1972; Henderson and Hilton 1974a; Henderson and Hilton 1974b). In those earlier reentry detections, three ships usually participated in the measurements during either ascent, reentry, or both, so that array capabilities were available if needed. In these earlier measurements, multiple microphones were closely spaced and were also carefully placed on individual ships so that for the high Mach number and nearly vertical arrivals, multiple reflections off the ship structures could be minimized (Hilton and Henderson 1972). Reentry speeds were similar to that of Genesis (~11 km/sec) and flight path angles (with respect to the local horizon) varied considerably from steep to shallow for these earlier entry tests.

Signal Detection and Analyses

We used the standard signal processing detection and location software, MATSEIS/Infra_Tool (available from Sandia National Laboratory) to analyze the data from our temporary three-element array in Wendover, Nevada. A conventional channel plot of amplitude versus time of the initial N wave arrivals is given in Fig. 4.

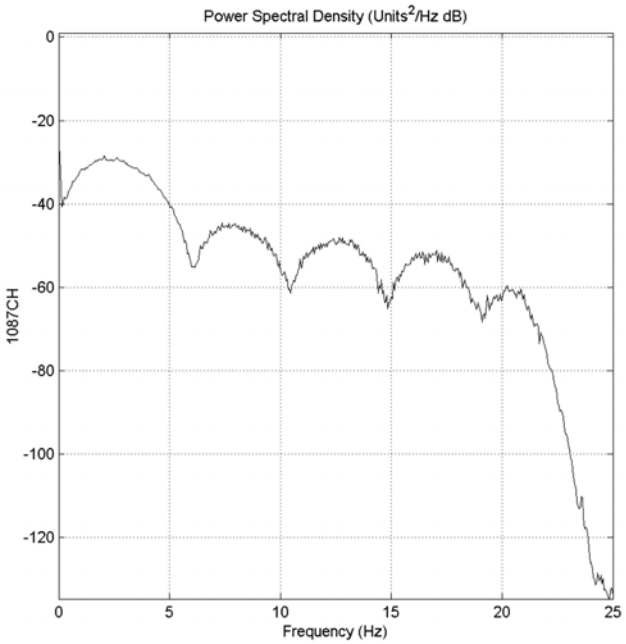

Fig. 5a. FFT power spectrum of the N wave arrival (for frequencies <25 Hz).

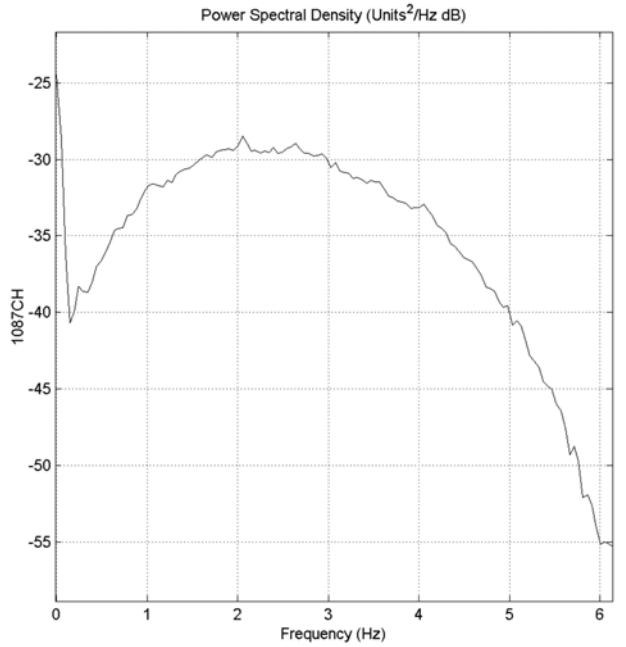

Fig. 5b. FFT power spectrum of the N wave arrival (for frequencies <6 Hz).

An FFT-based power spectral density (PSD) plot of the signal power is given in Figs. 5a and 5b (for frequencies <25 Hz and <6 Hz, respectively). A spectrogram of power levels versus frequency and time is indicated in Fig. 6. Similar to other well known PSDs of N waves, a multiple-lobed peaked FFT on the high frequency side of the main acoustic peak is clearly evident (Garrick and Maglieri 1968).

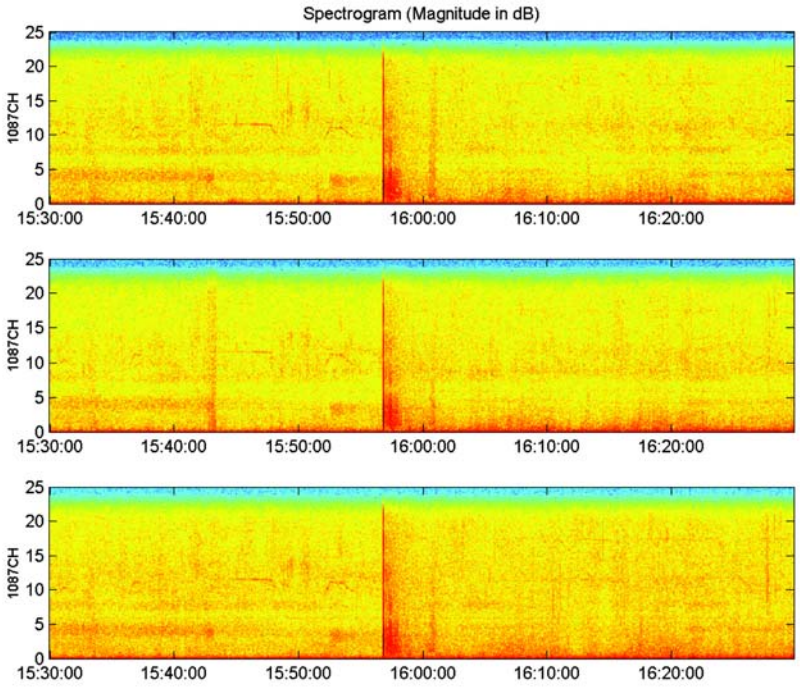

Fig. 6. Spectrogram.

The main "hypersonic boom" arrival occurred at approximately 15:57 UTC, which can be compared with the NASA nominal entry targeted at 15:55 UTC. This 2 min time delay corresponds to a total distance from the entry trajectory of about 37.9 km, roughly comparable to values used later below in our wave kinetic energy density conservation numerical approach. Based on peak heating at 15:53:46.25 UTC at about 60.323 km (at lat 41.2464°, long 244.2095°) as indicated by R. Wiens (personal communication 2004), the delay could be as much as 4 min, or a total range of 75.8 km. This puts a reasonable set of bounds on our wave kinetic energy density conservation approach for determination of the source altitude of the infrasonic signal arrivals.

On the basis of the observed Matseis/Infra_Tool signal trace velocity (≅0.583 km/sec, corresponding to an elevation arrival angle of 53.68° = $\cos^{-1}$ [c_s/V_{trace}]) coincident with the main "hypersonic boom" arrival at an assumed horizontal range from 26.1 km to 40 km (in order to bound the propagation problem), we can deduce a source height from 35.5 km to 54.4 km for a straight line ray path (unrefracted by assumption; see Figs. 7b and 7c with the corresponding vertical atmospheric structure parameters, i.e., the temperature and the two components of the mean horizontal winds plotted in Figs. 8a–8c) traveling downward from the rapidly moving point source. This is for the perpendicular point along the trajectory whereas as will be seen below the initial arrival is actually not from the perpendicular point, but at a greater source height back along the entry trajectory further to the west and south of Wendover. Here we have used the surface temperature of 296.65 K (sound speed = 0.3453 km/sec) to evaluate the elevation arrival angle). In the above expression, c_s is the adiabatic thermodynamic sound speed and V_{trace} is the horizontal trace velocity (the apparent speed with which the wave fronts cross the infrasound array horizontally). From these values, we can deduce a total travel distance of 44.0 km to 67.5 km, which for a mean sound speed of 0.316 km/sec (at a temperature of 296.65 K), yields time delays from 139.2 sec (≅2.32 min) to 213.7 sec (≅3.56 min), a value that fits quite nicely between our above travel time estimates.

We can also anticipate our results and determine the travel time for a "ray" corresponding to such heights and total range from the Genesis entry trajectory propagating downward from above to the Wendover airport. We have determined the answer to be ≅200–300 sec from a source height of 60 km for propagation through a multi-layered nonisothermal atmosphere, or 120–160 sec for a source height of 40 km, for example (see Fig. 7d). From our analysis just previous, this argues that the true source height is closer to 40 km than to 60 km. In addition, the Wendover airport is not at sea level, but at a geopotential height of z = 1.2914 km. This value must be subtracted from the above height estimates when comparisons are made using the wave kinetic energy density conservation approach, since those source height estimates are reckoned upward from the ground (z = 0). In practice, however, this only accounts for a decreased travel time of ~4.1 sec. In addition to this altitude correction relative to sea level, we have also corrected the array coordinates for the magnetic declination deviation of ~15° at Wendover. This nontrivial correction resulted in a plane wave

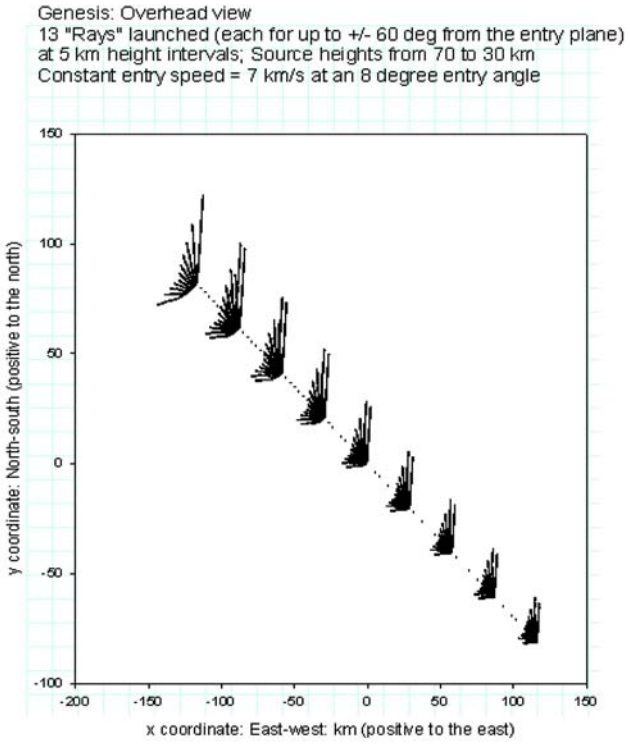

Fig. 7a. Wave normal analyses for a moving point source (viewed from above): "Rays" are launched every 5 km at 13 intervals with respect to the entry plane ($\Delta\phi \cong 0$ to +/– 60°) for source heights from 70 to 30 km.

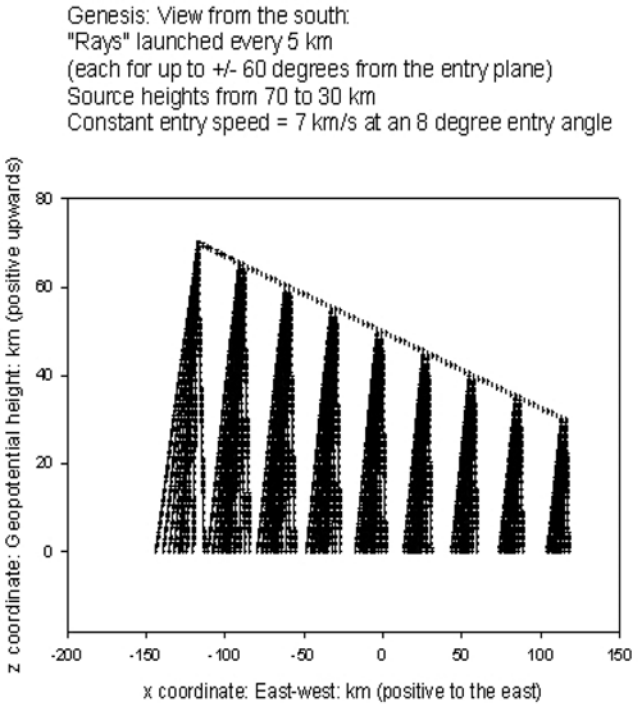

Fig. 7b. Wave normal analyses for a moving point source (viewed from the south): "Rays" are launched every 5 km at 13 intervals with respect to the entry plane ($\Delta\phi \cong 0$ to +/– 60°) for source heights from 70 to 30 km.

back azimuth using Infra_Tool (and also using standard seismic f-k analysis) that shifted from about 216.3° (uncorrected) to a final value for the initial N wave arrivals of ~220.2°.

When the Infra_Tool results (Fig. 9) are physically interpreted below, we have determined that the initial arrivals emanated from an intersection point on the trajectory about 44 km above sea level, based on the mean ray angle back to the entry trajectory measured from the Wendover infrasound array. A summary of the infrasound detections in Infra_Tool can be made as follows, in terms of the predicted, plane wave back-azimuth variations (Fig. 9):

1. The initial arrival of ~220° switching to 340° intermittently. We also saw such rapid azimuth variations from infrasound data collected in the western United States at five LANL infrasound arrays operated during the space shuttle Columbia disaster and shown in ReVelle et al. (2003).
2. A gradual, nearly linear return to ~220° (with some azimuth variation once again) back to the prevailing microbarom arrivals (just as it was before the Genesis signals arrived) to values of ~290°. Microbaroms, the atmospheric analog of the seismic signal microseisms, represent the prevailing background noise level in the atmosphere. They are propagating infrasonic signals originating from oceanic storms at a nearly

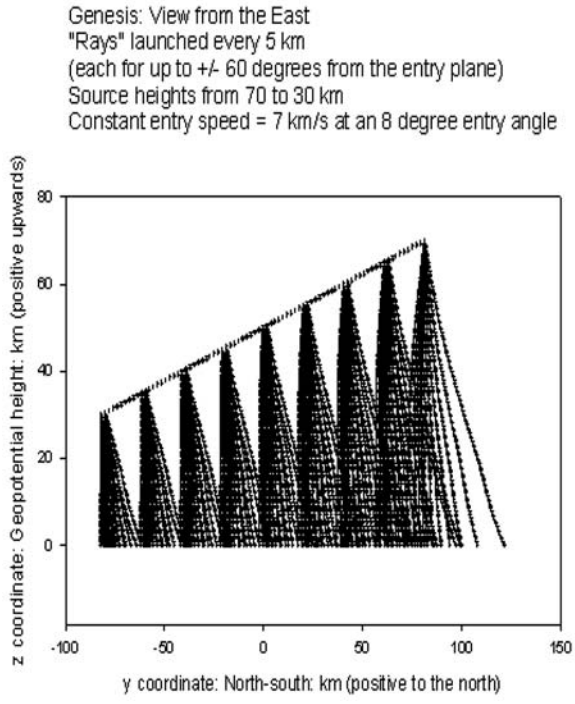

Fig. 7c. Wave normal analyses for a moving point source (viewed from the east): "Rays" are launched every 5 km at 13 intervals with respect to the entry plane ($\Delta\phi \cong 0$ to +/– 60°) for source heights from 70 to 30 km.

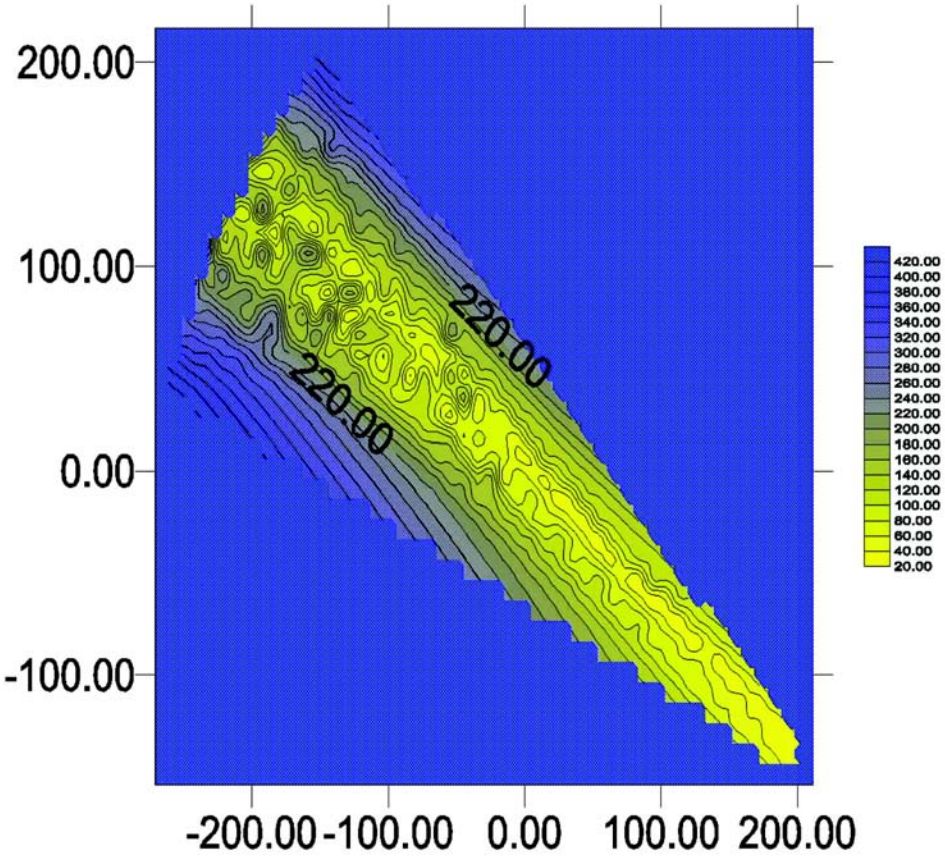

Fig. 7d. Overhead view in the {x,y} plane of the contours of the acoustic travel time to the first bounce condition (for the nominal Genesis "hypersonic boom" corridor with environmental parameters as plotted earlier).

monochromatic wave period of 5–7 sec. They are generated by low-pressure regions over the ocean by the interaction of atmospheric winds and the ocean surface, in terms of a standing wave pattern whose amplitude is almost always prevalent when other noise sources such as wind disappear.

3. A gradual increase of the back azimuth from 220° to 290°, turning back toward ~270° until the reflection signal arrives (after bouncing off a nearby mountain range) from ~90° with a linear decrease first to 75° and then decreasing to arrive from a more northerly direction after about 4 min since the first large amplitude hypersonic boom arrival.
4. A subsequent return to the prevailing microbarom arrivals at ~290°.

Finally, as shown in Fig. 10 by using the standard seismic frequency-wave number (f-k) location method, we have also independently determined a back azimuth of 220.7° for the initial hypersonic boom signals that arrived at the Wendover infrasound array. For this back azimuth, the intersection point along the entry trajectory is ~45 km, which is in quite reasonable agreement with the Infra_Tool approach (see Fig. 1b).

ACOUSTIC ENERGY AND RAY TRACING: WAVE NORMAL ARRIVALS

Atmospheric Structure Parameters

In order to ray trace the wave normal field, we needed the best possible atmospheric temperature (or sound speed) and horizontal wind speed structure available for September 8, 2004. This we provided by utilizing conventional U.S. Weather Service radiosonde ascent data from Salt Lake City and from the output of MSIS-E (Hedin et al. 1996), which is now updated and maintained by the U.S. Naval Research Laboratory (NRL) in Washington, D.C., as well as the HWM (horizontal wind model) (Picone et al. [2002]). These atmospheric structure parameters (mean values of the temperature and horizontal winds) are plotted in Figs. 8a–8c.

Top-Down–Bottom-Up Ray Tracing Validity Checks: Wave Normal Path Reconstructions

The results of standard wave normal wave normal ray tracing in Cartesian coordinates from a supersonic or even a

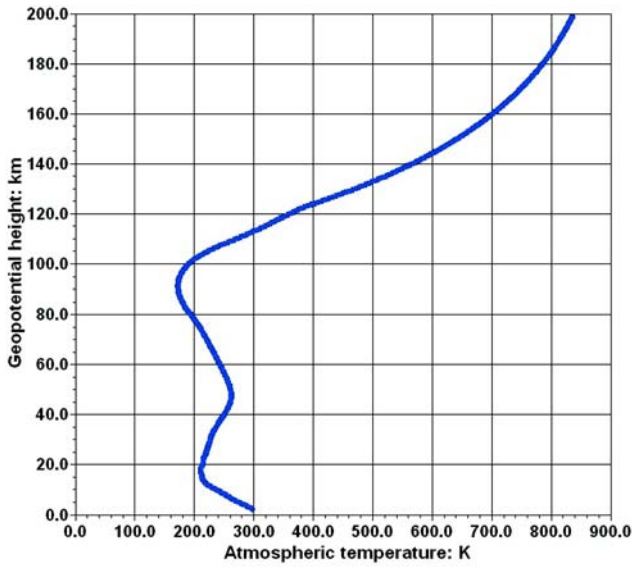

Fig. 8a. Atmospheric temperature structure with radiosonde data (0600Z, September 8, 2004) from Salt Lake City at the lowest heights and using MSIS-E above.

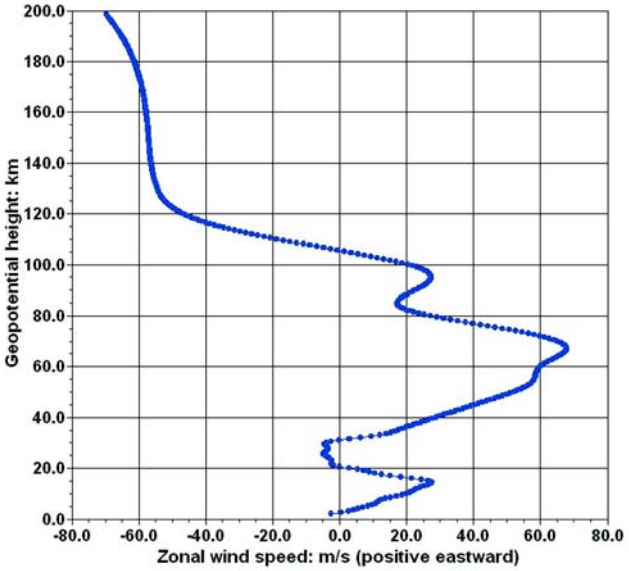

Fig. 8b. Atmospheric wind zonal structure available from the HWM model.

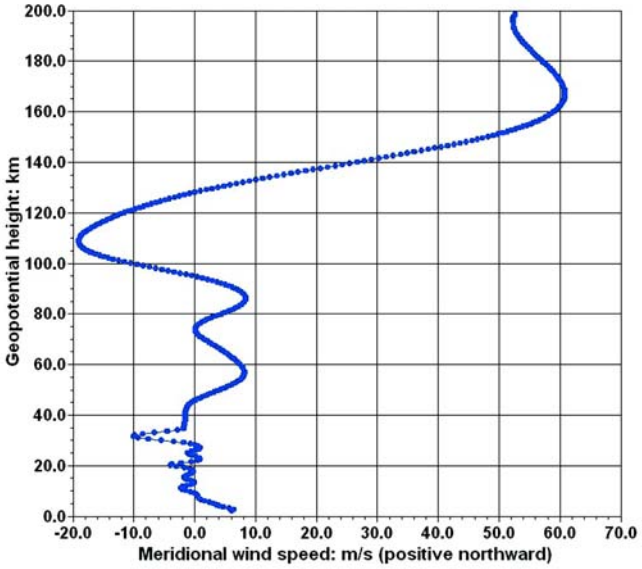

Fig. 8c. Atmospheric meridional wind structure available from the HWM model.

hypersonic source (ReVelle et al. 2004; and ReVelle Forthcoming) such as Genesis is provided in Figs. 7a–7c. At an entry angle of 8°, we are stretching the validity of the Cartesian coordinate system approach, but it has nevertheless been found useful previously, as it was also successfully applied to the Columbia shuttle reentry disaster of February 1, 2003 (ReVelle et al. 2003).

This approach is similar to the "wave normal" approach that was developed by Hayes et al. (1969), but we have typically assumed an infinite speed line source so that the complete phase reconstruction of the signals for a rapidly moving point source was not necessary (which in reality is what the Genesis reentry source actually is). Here we will compare these downward ray tracing results to those determined previously using Matseis/Infra_Tool, hence we are doing a top-down–bottom-up validity check on all of ray tracing solutions.

We can choose to utilize any of three readily possible options for the evaluation of the characteristic velocity of the acoustical waves as they propagate, namely:

- Ideal line source (infinite speed source, an assumed instantaneous energy release)
- Modified line source (as above, but with blast wave radii corrections for fragmentation)
- Supersonic line source with an explicit Mach cone half angle based on a constant speed with respect to sound waves.

For the Genesis reentry, it is the last option that is the most appropriate, given its very low entry speed in comparison with most normal meteor entries.

We have run a number of cases for the Genesis reentry, only the last of which we will report on here. This was for the following nominal set of entry parameters as follows: horizontal entry angle (mean) = 8° and mean entry speed = 7 km/sec (Mach cone half angle with respect to an isothermal, hydrostatic atmosphere = 2.59 deg, for a mean sound speed = 0.316 km/sec) on a vector heading of 125° (R. Wiens, personal communication 2004). For this vector heading, the perpendicular ray towards Wendover would have an azimuth launch angle equalling 35°. If the finite Mach cone angle is also put into the prediction, the resulting launch angle is

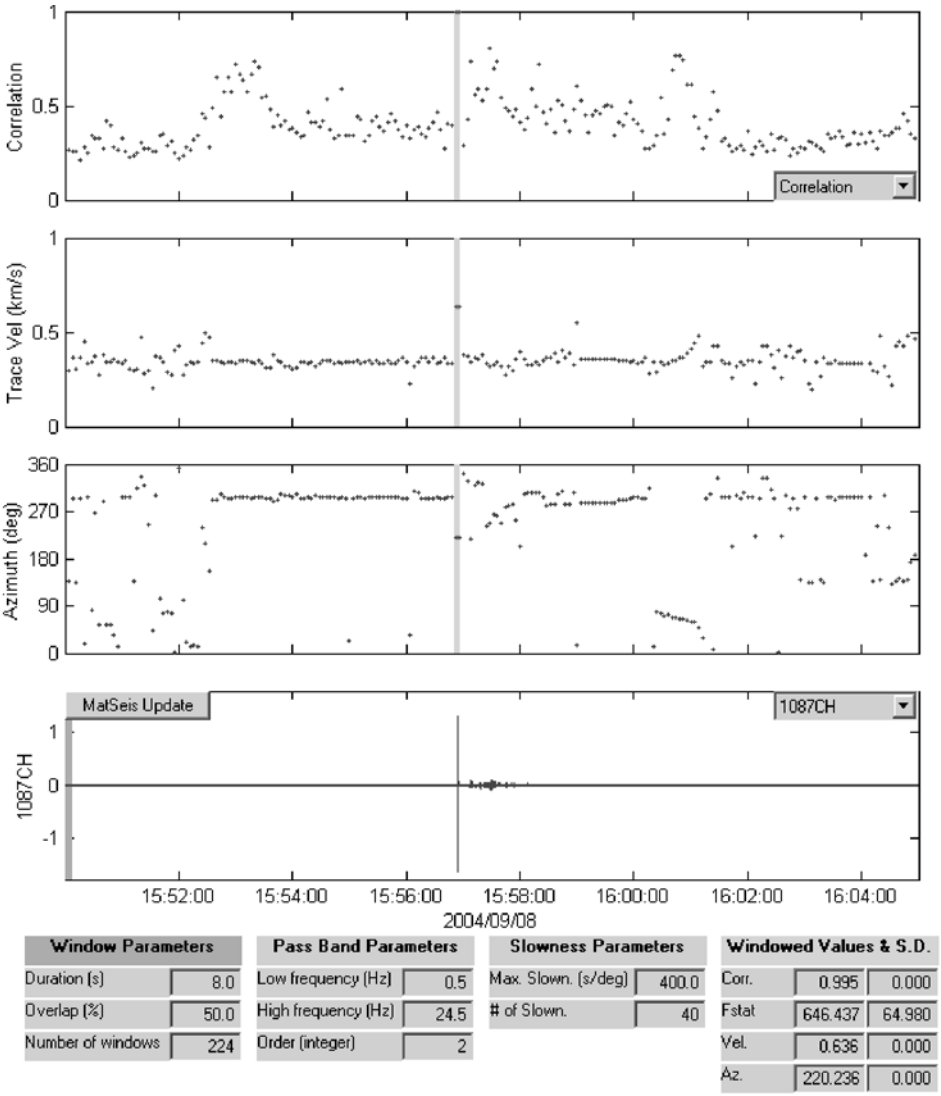

Fig. 9. MATSEIS: Infra_Tool Detection—Initial N wave arrivals and subsequent reflection off nearby mountains.

increased slightly (for a straight line path) to 37.59°. The wave normal ray tracing results are plotted below in Figs. 7a–7c. The predicted arrival angles for the position of our array at the Wendover airport with respect to the Genesis entry trajectory are as follows (including the Mach cone half angle effect):

- Initial azimuth arrival angle; vector heading angle = 37.6°
- Elevation arrival angle from a 60 km source altitude = 55°
- Propagation time delay = 180 sec (3 min)

These values can be compared with those generated during the signal detection and analysis work with Matseis/Infra_Tool, which are: plane wave back azimuth: 220.2° (= a 39.8° vector heading angle), trace velocity = 0.58 km/sec (53.7° elevation arrival angle), and lastly, the propagation time delay = 2–4 min. These are the final results after the corrections from geomagnetic north to geographic north were made (geomagnetic-geographic offset of ~15° at the Wendover airport monitoring location) agreeing perfectly with the ray tracing results and within ~2.2° of the simple Mach cone and entry trajectory heading results given just above, which assumes a strictly straight line path between the source and the observation point.

Given all of the uncertainties, all of the key quantities are within standard error bars computed internally for our results.

Differential Acoustic Efficiency Evaluations Assuming Wave Kinetic Energy Density Conservation (Inviscid Treatment)

The recently developed method used here is described in detail in ReVelle et al. (2004), and the mathematics will not be fully elaborated on again here. It is a numerical approach that conserves the wave kinetic energy density (assuming an inviscid medium at these low frequencies at relatively low

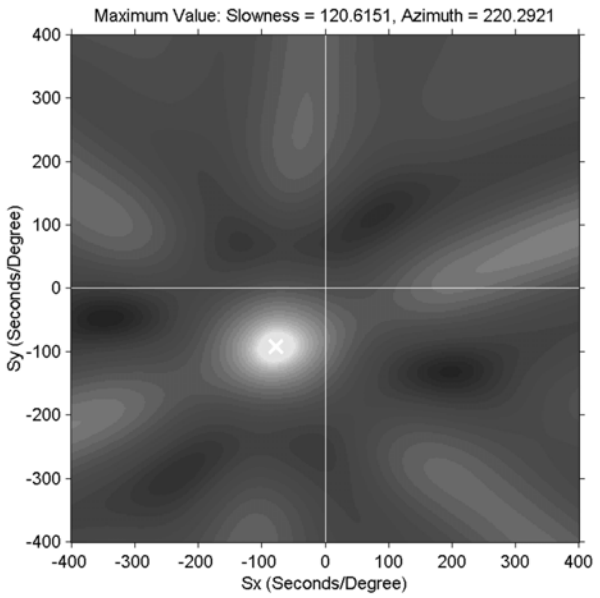

Fig. 10. MATSEIS: FK detection.

heights) by iterating the blast wave radius as a free variable (not using the linear, least squares curve fitted blast wave radius in Equation 1 below) until a match between the differential acoustic efficiency at the source and at the ground observation point are within a specified tolerance (we assumed a matching tolerance = 0.010%). This assumes a direct wave arrival, whose total range from the source can be adequately represented as the square root of the sum of the squares of the horizontal range and of the assumed source altitude. Both range dependencies and air density dependencies are accounted for in this iterative process for either weakly nonlinear or strictly linear acoustic wave propagation, the effects of which are also explicitly allowed within the iterative numerical algorithm. This procedure was originally developed and tested for an isothermal, hydrostatic atmosphere, but the entire process was modified for this paper to fully account for a non-isothermal atmospheric density and sound speed structure and their variability with altitude (which effectively reproduces the U.S. Standard Atmosphere [1966] in either the summer or winter months at middle latitudes).

After reconstructing the Genesis entry using the approach described earlier in this paper, we have determined the following linear, least-squares curve fit parameters over the entire trajectory, all with the geopotential altitude z expressed in km (derived from the detailed entry dynamics solutions determined above):

Blast radius (in m): $r^2 = 0.9999$ m

$$R_o(z) = y_o + az + bz^2 + cz^3 \quad (1)$$

where $y_o = -53.81$, $a = 3.603$, $b = -6.085 \cdot 10^{-2}$, and $c = 3.510 \cdot 10^{-4}$. This curve fit solution is not used in the iterative wave kinetic energy conservation algorithm described below, but was used in the computation of the source energy using method B in Table 4 by matching the predicted wave period compared to the observed wave period at the ground as a function of horizontal range and height.

Velocity (in km/sec): $r^2 = 0.9993$ km/sec

$$V(z) = y_o + az + bz^2 + cz^3 \quad (2)$$

where $y_o = -30.24$, $a = 1.999$, $b = -3.248 \cdot 10^{-2}$, and $c = 1.757 \cdot 10^{-4}$.

Kinetic energy (in J) : $r^2 = 0.9960$ J

$$KE(z) = y_o + az + bz^2 + cz^3 \quad (3)$$

where $y_o = -2.924 \cdot 10^{10}$, $a = 1.489 \cdot 10^9$, $b = -1.569 \cdot 10^7$, and $c = 4.470 \cdot 10^4$.

Since the differential acoustic efficiency concept and calculation procedure is still quite new, we will very briefly repeat the development in ReVelle et al. (2004) and in ReVelle (Forthcoming).

Differential Acoustic Efficiency Definition

The near-field differential acoustic efficiency, ε, can be evaluated by forming the ratio of the weak shock, acoustic wave kinetic energy density (at x = 10) compared to the bolide kinetic energy density being deposited within the nonlinear source volume region defined at x = 1, where $x \equiv R/R_o$, R = slant range from the bolide and R_o is the line source/modified line source blast wave relaxation radius.

Therefore, let ε ≡ wave kinetic energy density/kinetic energy transferred into the nonlinear source deposition volume

$$\therefore \varepsilon(z) \equiv \frac{1}{2} \cdot \rho(z) \cdot \Delta u^2(z) / \quad (4)$$

$$\left\{ \frac{1}{2} \cdot m(z) \cdot V(z)^2 / \pi \cdot R_o^2(z) \cdot l(z) \right\}$$

where $\Delta u = \Delta p(z)/\{\rho(z) \cdot c_s(z)\}$ for plane acoustic waves (wind due to the wave), $m(z)$ = instantaneous meteor mass as a function of the geopotential source altitude, $p(z)$ = ambient pressure as a function of altitude, $\rho(z)$ = ambient air density as a function of altitude, $l(z)$ = line source length as a function of altitude, ε evaluated at x = 10 (= 10 · R_o from the entry trajectory), where $\Delta p(z) = 0.05750 \cdot p(z)$ from "first principles," theoretical numerical line source pressure wave calculations as discussed in ReVelle (2002a; Forthcoming).

All of the first principles line source blast wave solutions were done using numerical results given in Plooster (1968, 1971), which were all originally done for studying lightning

Table 3. Genesis: Measured infrasound signal properties.[a]

Maximum amplitude: Pa	3.9995 ± 0.1585
Peak to peak amplitude: Pa	7.2625 ± 0.317
Prior noise (RMS amplitude):	$2.25 \cdot 10^{-3} \pm 1.25 \cdot 10^{-3}$
Post noise (RMS amplitude):	$6.50 \cdot 10^{-3} \pm 4.00 \cdot 10^{-3}$
Integrated signal energy:	
Bolide signal	93.303 ± 4.971 Pa^2
Prior background noise	0.019375 Pa^2
Post background noise	0.19250 Pa^2
Mean background noise	0.10625 ± 0.01375 Pa^2
Standard deviation of mean noise between prior and post energy	$1.224 \cdot 10^{-1}$ Pa^2
Signal to noise ratio (peak to peak ratio)	Bolide SNR: 3227.8 ± 253.6
Dominant signal frequency	2.2461 (FFT) ± 0.1382 Hz[b]
Dominant signal period	0.4452 (FFT) ± 0.0275 sec[b]

[a]After converting raw amplitudes in digital counts using a) $3.77 \cdot 10^{-6}$ microbar/count, b) 0.04 V/microbar or 400 mV/Pa; 1 microbar = 0.10 Pa, and c) band-pass utilized: 0.50 to 24.5 Hz[b].

[b]In order to determine the mean wave period, an FFT of the signal was utilized. Standard zero-crossing techniques did not work reliably in this case, probably because of our inability to reliably define the return to zero of the signal, i.e., to ambient pressure conditions.

discharges in a very high temperature environment in the lower atmosphere.

Our least squares curve-fit evaluation of the differential acoustic efficiency for the Genesis reentry is now presented below. Differential acoustic efficiency (dimensionless): $r^2 = 0.9999$

$$\varepsilon_a(z) = a \cdot \exp\{-bz\} \quad (5)$$

where $a = 7.794 \cdot 10^2$, $b = 0.1645$; 1/b ~ Hp (≅6.079 km), and where H_p = pressure scale height of the isothermal, hydrostatic atmospheric model.

Following ReVelle et al. (2004), we have matched the wave kinetic energy density at the ground (using the observed infrasonic waves) to that at the source at x = 10 (10 blast wave radii away from the entry trajectory which varies as a function of height due to the atmospheric-"meteor" interaction). This was done by physically iterating the blast radius as a free parameter until the acoustic efficiency at the ground matched the value at the source after corrections were applied for source altitude, range, wave propagation type, i.e., linear or weakly nonlinear, and so forth. Possible solutions are presented in Figs. 11b–11d for both the resultant blast radius and source kinetic energy (expressed in kt, where 1 kt = $4.18 \cdot 10^{12}$ J) for the same assumed horizontal range (=40 km), but for different versions of the differential acoustic efficiencies (see below). Source heights were finally determined (see Table 4) if the iterated free variable blast radii exactly matched the entry dynamical predictions of the computed line source blast radius as a function of height deduced earlier for Genesis in the Prediction of the Genesis Entry Environment section. In Table 4, we also list the key properties for the Genesis infrasonic signals, using exactly the same set of methods as used recently to analyze infrasonic signals from the Neuschwanstein meteorite fall (ReVelle et al. 2004), but this time with an explicit allowance for curve-fitted linear, least squares velocity values as a function of the geopotential height.

The computed differential acoustic efficiency became quite large in our analyses (Fig. 3) and even exceeded initially 100% below about 40.7 km. We believe that the fundamental cause of this unphysical behavior is the fact that we are utilizing very high Mach number (line source hypersonic flow) relations to connect the resulting blast wave overpressure to the various entry source parameters. At these low Mach numbers, the supersonic flow theory relations should really be used instead. Details for this development can be found for example, in Whitham (1950), Hubbard et al. (1964), and Hayes et al. (1968), and are also indicated briefly below.

Even after making these simplified corrections (discussed below), at geopotential heights less than ~27 km, an exponential decay smoothing factor was applied to allow each parameter to return back toward more reasonable reduced physical magnitude values. In fact, for the nominal (uncorrected) acoustic efficiency results, if this exponential decay factor was not applied, no low-altitude solutions were evident at all, implying that the decrease in $\varepsilon_a(z)$ with decreasing altitude was a necessary condition for obtaining solutions at low heights. Nominal solutions at heights above ~88–97 km were found, however, as indicated with the results plotted in Fig. 11b.

Since the above hypersonic flow theory solutions were not completely satisfactory, we decided to investigate the possible root causes of the very large differential acoustic efficiencies at the lowest velocities of the Genesis probe during reentry. Using the standard equation for the overpressure produced far from the axis of a supersonic body of revolution (Whitham 1950), we can compare the hypersonic line source theory pressure wave amplitude prediction (ReVelle et al. 2004) to that for a moving point source in supersonic flow with the following parameters at the same altitude and distance from the event (assuming $d = L$, where L = vehicle length and d = vehicle cross-sectional diameter):

$$\Delta p_{hyper} / \Delta p_{super|M>1} \propto \left[\{p(z) \cdot p_o\}^{\frac{1}{2}} \cdot \{R_o / R\}^{\frac{3}{4}}\right] / \left[\{p(z) \cdot p_o\}^{\frac{1}{2}} \cdot \{M^2 - 1\}^{\frac{1}{8}} \cdot d^{\frac{3}{4}} / R^{\frac{3}{4}}\right] \quad (6)$$

In Equation 6, we have assumed that the altitude term and its dependence in the standard supersonic source relationship can in general be replaced by the total slant range R and where p(z) is the atmospheric pressure as a function of height with p_0 equal to the surface air pressure. In addition, we have

Table 4. Genesis numerical solutions: Kinetic energy density conservation approach (1 kt = $4.185 \cdot 10^{12}$ J); search interval = 1.0 km; Surface air density = 1.225 kg/m^3; infrasound evaluations: Nominal differential acoustic efficiency with two additional solutions whose acoustic efficiencies were reduced by 4 and 10 times (see method E).

Type of approach	Main infrasonic arrival
R_{obs} = 26.1 km (slant range) for z = 43.07 km: NASA pre-entry nominal, closest horizontal range, and source height	τ = 0.4452 sec (FFT), Δp = 3.9995 Pa
[a]$E_{so} = 1.3607 \cdot 10^{10}$ J $= 3.2514 \cdot 10^{-3}$ kt	y = ½: linearized, geometrical acoustics ray propagation regime
	d' = 111.9 km
[b]Method A: E_s	$= 3.53 \cdot 10^{-4}$ kt
[c]Method B: E_s^i	$= 5.09 \cdot 10^{-4}$ (range = 26.1 km) to $= 3.32 \cdot 10^{-4}$ kt (range = 40 km)
[d]Method C: E_s^i	$= 8.52 \cdot 10^{-4}$ (range = 26.1 km) to $= 5.09 \cdot 10^{-4}$ kt (range = 40 km)
[e]Method D: Source height: km	z = 48.1 km (range = 26.1 km) to z = 40.9 km (range = 40 km)
[f]Method E: At 26.1 km range (40 km range solutions in parentheses)	Multiple solutions: z = 9–14 (11–15.5) km and for z = 88–98 km
[g]Method E: At 26.1 km range (40 km range solutions in parentheses)	Multiple solutions: z = 15–20 (16.5–21) km and for z = 77.5–86 km
[h]Method E: At 26.1 km range (40 km range solutions in parentheses)	Multiple solutions: z = 19–24 (20.5–25) km and for z = 71.5–79 km

[a]Initial pre-atmospheric kinetic energy for a 225 kg mass moving at 11.0 km/sec.
[b]USAF Technical Applications Center, Patrick Air Force Base, Florida (observed wave period only).
[c]Line source (observed wave period and range only).
[d]Line source (observed wave amplitude and range only) at the predicted source height listed below in Method D.
[e]Line source (observed period, amplitude and range): isothermal atmosphere.
[f]Iterative line source blast wave radius (kinetic energy density conservation): R_o = 10–30 m, Nominal acoustic efficiency (hypersonic flow modeling).
[g]Iterative line source blast wave radius (kinetic energy density conservation): R_o = 10–30 m, Uniform reduction of computed acoustic efficiency results by 4 times.
[h]Iterative line source blast wave radius (kinetic energy density conservation): R_o = 10–30 m, Uniform reduction of computed acoustic efficiency results by 10 times.
[i]Unlike previous treatments ReVelle et al. (2004) where these two values have been identical at a specified fixed horizontal range, we have now allowed the velocity to vary as predicted theoretically (using the linear least squares, curve-fitted velocity).

assumed that $R_0 = M \cdot d$ = line source blast wave relaxation radius (ReVelle et al. 2004) as applicable for the case of no fragmentation. After cancellation of terms, we have the following useful result:

$$\therefore \Delta p_{hyper} / \Delta p_{super|M>1} \propto M^{\frac{3}{4}} / M^{\frac{1}{4}} = M^{\frac{1}{2}} \quad (7)$$

that is ~O(4) at M = 20 (with O() meaning order of magnitude). Thus, supersonic pressure wave amplitudes, with all else the same, are expected to be consistently smaller than the hypersonic values, which certainly seems very physically plausible. A physical construction linking these two results as a function of Mach number is certainly a topic that needs to be pursued for such low-speed entries. Thus, as time gets larger in Fig. 3, the slope of the differential acoustic efficiency should become progressively less steep, i.e., "flatter," and then the total power balance will then more closely approach 100% at low heights. This comment is applicable to bolide modeling as well, especially with regard to meteorite entry where quite low speeds are typically encountered at the lowest model entry heights so it is not just an item of academic interest.

Note that, in general, the expected reduction in the magnitude of the differential acoustic efficiency is not uniform with height, since it is expected to change with the local Mach number of the flow. We present results below for both extreme options, however, i.e., a standard, nominal line source blast wave theory differential acoustic efficiency result at all heights/times and two additional results that have been reduced uniformly according to the above evaluations relative to standard supersonic flow theory predictions by a factor of either 4 or 10 times, respectively. It is to be noted that this correction does, however, make a rather large difference in the self-consistency and thus in the overall improvement of our solutions. In addition, at very low Mach number, the supersonic wave drag coefficient also becomes slightly larger compared with hypersonic flow values, making the drag interaction larger and an associated larger blast wave radius, once again with all else the same. In addition, as shown by Whitham and others, the corresponding positive phase duration of the waveform (half the wave period for an ideal N wave) also changes its various dependencies for supersonic as compared to hypersonic flow sources, but these changes have not yet been addressed here, either.

The range source height data for the position of the Genesis spacecraft with respect to our infrasonic array in Wendover, Nevada, is indicated in Fig. 11a, and was provided to us by W. Cooke and colleagues at NASA Marshall Spaceflight Center, Huntsville, Alabama. The results are given in Figs. 11b–11d for the nominal hypersonic differential acoustic efficiency case and for the case with a uniform

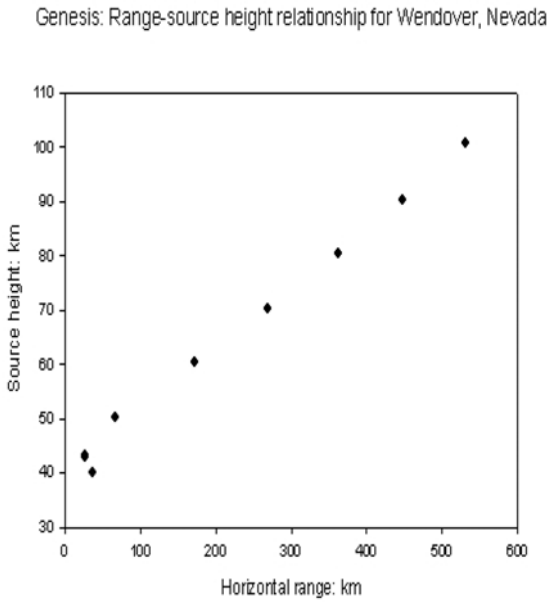

Fig. 11a. Genesis: range-source height relationship for the infrasonic array in Wendover, Nevada.

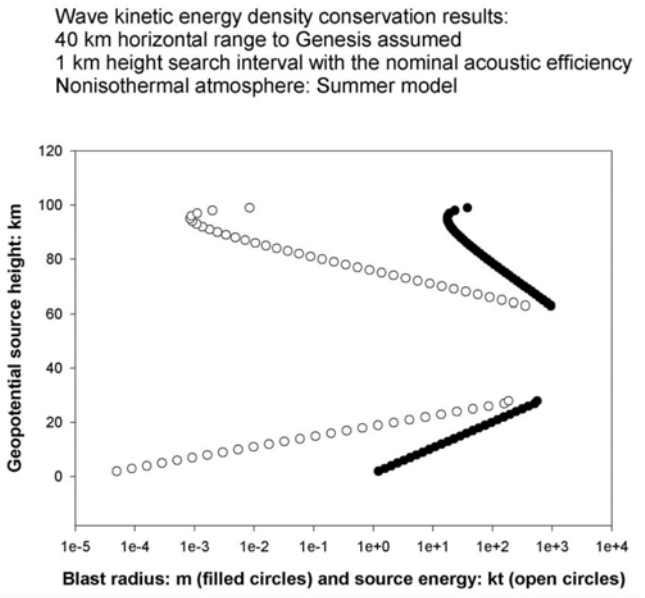

Fig. 11b. Source altitude search with infrasonic data: nominal acoustic efficiency results.

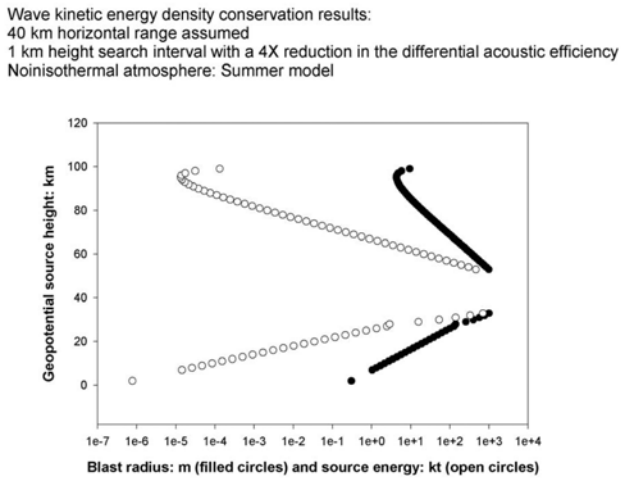

Fig. 11c. Source altitude search with infrasonic data: acoustic efficiency results uniformly reduced by four times.

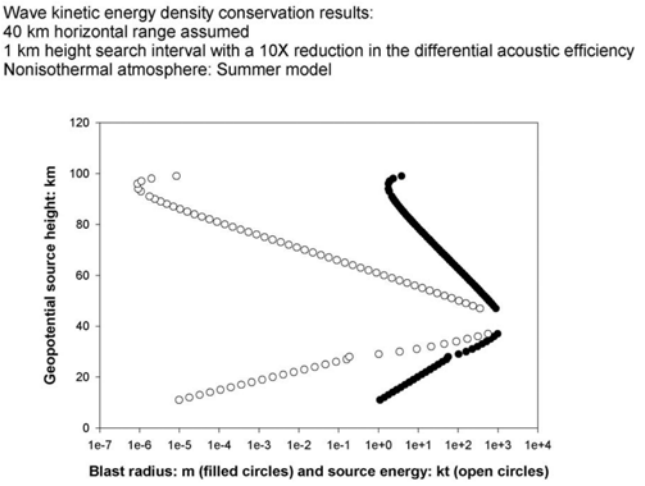

Fig. 11d. Source altitude search with infrasonic data: acoustic efficiency results uniformly reduced ten times.

reduction by a factor of 4 and 10 times, respectively (in comparison with the nominal line source blast wave differential acoustic efficiency results). All plotted results are for a range of 40 km (rather than the nominal entry trajectory range of 26.1 km), which is still quite close to the corresponding point of closest approach to the entry trajectory. We view the 40 km range solution as a possible perturbed range (a range deviation of some 14 km larger than the nominal NASA value), which is probably an upper limit to the possible range deviation during the final entry phase (see also below).

During these evaluations of all of our results, shown in Figs. 11b–11d and in Table 4 (the table has mostly evaluated the consistency of the wave kinetic energy density conservation solutions at the nominal NASA range of 26.1 km), we have consistently utilized the FFT spectral peak of the signal (~0.443 sec) rather than the conventional period at maximum signal amplitude. This was done because of technical problems in reliably measuring the standard zero-crossing technique of the wave period (probably because of lengthy negative phase returns and defining these precisely with respect to ambient conditions for each of the three infrasonic pressure wave sensors detecting the Genesis signals; see the offset of zero pressure evident in Fig. 4 following the initial N wave arrivals).

Tests were performed by D.O.R. to evaluate the ability of

the Fourier transform approach to reliably reproduce the input duration of a finite duration ideal N wave type signal (as well as for a saw-tooth input wave of infinite duration). It was found that the Fourier transform approach could reproduce the initial duration of the waveform to be within 5–10% of the input value. Standard zero-crossing results were consistently up to a factor of two longer in their averaged deduced wave period and with a correspondingly larger set of internally measured error bars as well (depending on the band-pass frequency range that had been chosen). This study was undertaken because for the zero-crossing dominant wave frequency results, we obtained wave kinetic energy density conservation results that were totally unphysical, i.e., the source energy estimates exceeded the known original source energy values (for a zero-crossing wave period of ~0.748 sec). Since we have now verified the ability of the FFT to fully and reliably reproduce input wave durations and dominant wave frequencies as we transformed back and forth between the time and the frequency domains, we have only utilized the FFT frequency results in our wave kinetic energy density solutions for Genesis.

In an effort to fully understand these earlier unphysical solutions, we have also tried additional solutions at larger horizontal ranges up to 100 km and corresponding to higher source heights (using the wave kinetic energy density conservation technique), and these did improve the solutions (both with the nominal hypersonic acoustic efficiency as well as with a uniform reduction factor of 4 and 10 times, respectively). Solutions using a horizontal range of 50 km from Wendover airport are probably an upper limit to the true deviation of the final entry path from the nominal NASA range value, however. This is because our standard blast wave height solutions that utilize both observed wave amplitude and period data (for details see ReVelle et al. 2004) progress downward from 48.9 to 40.9 to ~37.2 km for assumed horizontal ranges from 26.1 to 40 to 50 km, respectively. From all of the other constraints discussed earlier, it appears that source heights below 37 km or above 46 km are not very probable.

Still, these various horizontal range solutions have to also match the observed back azimuth found from Matseis/Infra_Tool and from the line source ray tracing as well, that is, range is not a totally free parameter in these calculations. The Genesis Mach cone at low altitudes is substantially wider than for most high-velocity meteors and so the point of closest approach (in altitude and range) is not necessarily the point from which the initial "hypersonic boom" at Wendover originated due to the finite Mach cone half-angle.

All of these solutions determined so far all are in the "linear" acoustic propagation regime. In addition, all of our solutions have been calculated, assuming that $R_o << H_\rho$, i.e., a "small" source compared to the local density scale height for a hydrostatic, nonisothermal model atmosphere. Any solutions for which this was not the case were automatically rejected in our numerical algorithm (this is why our solutions appear to terminate abruptly at very large blast wave radii ~10 km). Multi-valued numerical solutions have been determined in two distinct branches in general, one at high altitude and one at low altitude. The upper, higher altitude branch, can be characterized by a blast radius and an air density (or atmospheric pressure) and a relatively small differential acoustic efficiency. The lower altitude branch can be categorized by the same blast radius and an increased air density (pressure) and a significantly larger differential acoustic efficiency predicted in the entry modeling (and presented in Fig. 2g). In some cases, the height transition of these quantities is smooth with a distinct maximum, as was the case for the stronger infrasonic signals for the entry of the Neuschwanstein bolide. This is certainly not always the case as is evident from our solutions for the Genesis entry because the result depends significantly on all of the determining factors such as range, height, nonisothermal atmospheric model parameters, wave period, wave amplitude, and so forth.

For the nonlinear acoustic wave regime to be a determining factor for Genesis, we have formally calculated that we would have had to have been at least 112 km away from the entry trajectory with our recorded values of the Genesis hypersonic boom, much further than we can possibly justify, given all of our earlier remarks in the Signal Detection and Analysis section. Interestingly, as we examined all possible solutions for this case, those at longer horizontal range (with nonlinear decay properties for range >112 km) done using our nominal hypersonic differential acoustic efficiency values completely mimic solutions at much closer range with reductions in the nominal acoustic efficiency, an observation that is certainly very physically meaningful.

There is yet another puzzle, however. In our recent kinetic energy density conservation work on the Neuschwanstein bolide (ReVelle et al. 2004), we found a solution set similar to the above solutions for the so-called "weaker" set of infrasound signals from the Neuschwanstein bolide. These weaker solutions were for signals that could be categorized, based on their pressure amplitude and on their wave period to be propagating weak shock waves, whereas the current signals from Genesis, although they have similar altitude kinetic energy density conservation solutions, are definitely in the linearized wave propagation regime. Although the stronger signals from Neuschwanstein were readily understandable, the weaker set of signals from Neuschwanstein did not produce a consistent solution set using the wave kinetic energy density conservation theory. Similarly, if we fix the range to the minimum value and keep all variables the same except for raising the amplitude of the Genesis signals by ~5 times (but certainly not justified since we accurately know the amplitude calibration factor for these data), all values are now reconcilable as with the "strong" signals from Neuschwanstein. However, this is definitely an area of research that needs further examination.

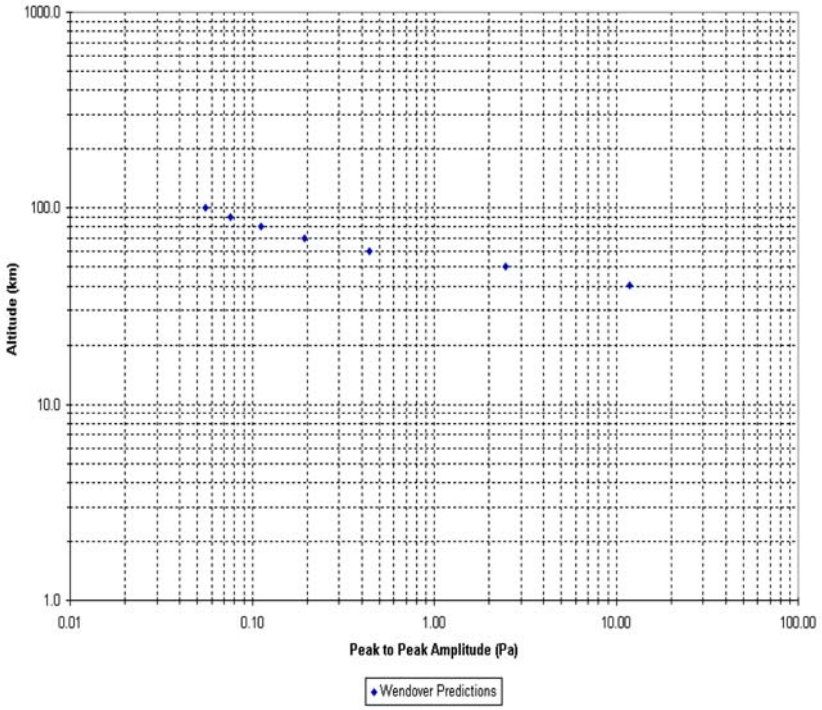

Fig. 12. Semi-empirical bolide solution: amplitude as a function of source altitude (km) and peak to peak pressure (Pa) for horizontal range from Wendover, Nevada from the Genesis entry trajectory.

Wave focusing, i.e., nonlinear amplitude enhancements (through wave front constructive interference effects), may account for some of these discrepancies and this effect has not been currently accounted for in our simple, direct numerical approach. In addition, the line source blast radius concept is strictly applicable to predicting pressure wave from an entry if it occurs with essentially zero deceleration. This is also clearly not the case for such low-speed surviving bodies. These and other possible effects will be more carefully investigated in the near future.

Finally, in Fig. 12, we compared the semi-empirical bolide solutions of Edwards et al. (Forthcoming) with the wave kinetic energy density conservation numerical predictions in Figs. 11b–11d. As can be seen the Edwards et al. (Forthcoming) approach demands a source height in the range from 40–50 km, precisely in a region where our wave conservation solutions are converging in the two branches (with one branch at low altitudes and the other one at high altitudes). This deduced height range is also in good agreement with the "wave normal" ray tracing solutions as well as with the Matseis/Infra_Tool solutions found earlier as well.

We are still awaiting a final NASA trajectory from the Jet Propulsion Laboratory and from the NASA Langley Research Center, but even in its absence, we have been able to determine theoretical wave kinetic energy density solutions as a function of range, wave period, and amplitude that matches the pre-entry "nominal" entry trajectory data (and for relatively minor range perturbations about that nominal solution). We have also utilized these "nominal" data in our analyses of the line source ray tracing of acoustical energy dispersion about that "nominal" entry trajectory.

Seismic Data Searches

After the crash of the Genesis capsule in the Utah Test and Training Range at 15:58:52 UT, it was immediately thought that nearby seismic instruments may have recorded surface waves generated by the impact, or possibly the ground motion associated with the passage of the hypersonic shock front analogous to previous seismic observations of supersonic aircraft and space shuttles (e.g., Cates and Sturtevant 2002; Kanamori et al. 1992). Although the seismic network surrounding the Genesis reentry trajectory is sparse (Fig. 1b), several stations did lie close (within ~50 km) to the ground projection, comparable in range to the temporary infrasound station at Wendover.

Unfortunately, the seismic stations of interest (ELK, FSU, DUG, and BGU) were operating with event detection algorithms at the time of the Genesis reentry. That is, only those data meeting the criteria of an earthquake (or other ground motion of interest) were recorded and saved. It is because of this that at the anticipated arrival times for the impact and airwaves at these stations, no data was available. Thus it appears that there are two possible explanations for this lack of recorded data: either 1) the induced ground motion for these sources were of such low amplitude that they did not trigger the recording of data, or 2) ground motion was

observed as it passed by these stations, but did not meet the criteria needed to cause the data to be saved. In hindsight, the former is likely the best explanation for any impact generated surface waves, as a 225 kg object impacting the surface at a speed of 311 km/hr would likely only produce observable surface waves in the immediate vicinity of the impact site as the equivalent energy is only that of a small sub-kilogram charge of TNT. The latter explanation is thought to be more likely for the lack of a seismically recorded airwave, as previous shock front observations have been made at comparable ranges, in more complex environments, for much less energetic aircraft.

SUMMARY AND CONCLUSIONS

Predictions and Measurements

Using an entry model developed by ReVelle (2001, 2002, Forthcoming) and by ReVelle et al. (2004), we have predicted the complete entry dynamics (drag and deceleration, etc.) and associated mass loss (with a concomitant prediction of the ablation parameter and various heat transfer coefficients) and heating rate as well as panchromatic luminosity, etc. of the entry of an artificial, albeit low-velocity, "meteor" fall and recovery at Dugway Proving Grounds in Utah, namely the entry of the Genesis space capsule after its nearly three year mission in space (with entry at about 9:57 am MDT on September 8, 2004). A standard three-element, infrasound array of pressure sensors was also rapidly deployed at the Wendover, Nevada airport after its transport there from Los Alamos (with a 3 dB band-pass for frequencies from ~0.02–300 Hz, while we have used a digital sampling rate of 50 Hz). This array allowed us to detect, locate, and categorize the "hypersonic" infrasonic boom from the reentry of the Genesis spacecraft. We have also used these detailed properties of the Genesis infrasonic "hypersonic boom" by connecting the various key measurements (amplitude, period and range, etc.) back to the source. This was done using the line source blast wave relaxation radius and the corresponding differential acoustic efficiency parameter that was predicted by relations developed from our previous hypersonic entry modeling work for large bolides. This differential efficiency was predicted as part of our theoretical entry modeling and was least squares curve fitted over the altitude penetration range for comparison with Genesis hypersonic boom amplitude and period levels, and so forth.

We have also independently determined the detailed paths of the wave normals for a hypersonic line source from a local Mach cone consistent with an average speed of Genesis during entry. This has also allowed us to connect together our wave signal processing results with results derived aloft using a top-down–bottom-up type of approach. An important result that was determined as a result of this study is that our previously determined differential hypersonic acoustic efficiencies needs to be adjusted systematically downward in its magnitude due to the decreased pressure amplitudes predicted by supersonic as compared to hypersonic flow theories. The transitional expression to accomplish this reduction will soon be developed as a direct result. We note finally that the predicted panchromatic magnitude for Genesis, again made on the basis of previous bolide modeling calibrations, was about −9, some three magnitudes less bright than the full moon. Preliminary comparisons with video data taken by A. Hildebrand and M. Beech confirm this brightness prediction.

Future Work: Stardust and Hayabusa

In January 2006, the Stardust spacecraft is scheduled for reentry over Dugway, Utah, and in 2007, the Japanese spacecraft Hayabusa is predicted to reenter over Australia. These manmade capsules were summarized in Table 1. We hope to once again be able to field one or more infrasound arrays for at least one of these smaller entry events and to further evaluate artificial, albeit low-velocity, meteor entries. One advantage of the Stardust reentry is its slightly higher entry velocity, albeit with a somewhat smaller capsule size than for Genesis, as is also the case for Hayabusa. These should also prove to be very good tests for a systematic examination of our previously determined bolide relations at the low-entry velocities more typical of meteorite entry and recovery efforts. This is especially the case from the panchromatic semi-empirical luminous efficiency, which has been largely calibrated by meteors at much larger entry velocities.

Acknowledgments–First and foremost, I would like to thank Mr. Tom Sandoval and Mr. Mel Garcia, both formerly of the Earth and Environmental Science Division at Los Alamos National Laboratory, for both calibrating as well as transporting equipment from Los Alamos to Wendover, Nevada, and for deployment of the field instrumentation on a very short time schedule. Without their great effort on Labor Day 2004, none of this work would have been possible. I would also like to thank Mr. Sandoval for doing the local GPS measurements of the infrasound array and computing the various separation baselines between the three pressure sensors. Finally, we would like to acknowledge the support of Dr. John Szymansky and Mr. Mark Hodgson of the Los Alamos National Laboratory (LANL), ISR-Research and Development Office for providing part of the funds needed to perform these measurements also on relatively short notice. Part of the funding for this ground-based effort was executed as part of the Genesis Hyperseed Multi-Instrument Aircraft Campaign (Peter Jenniskens, P.I., NASA Ames Research Center), and sponsored by the NASA Engineering and Safety Center. Discussions between D. O. ReVelle and Dr. Roger Wiens, one of the chief mission scientists on the Genesis

science team of ISR-1 of LANL, both prior to as well as after the entry, proved very useful as well. Finally, D. O. ReVelle greatly benefited from an electronic slide presentation given by Dr. D. Burnett (Misssion_status.ppt consisting of 47 slides) at the Jet Propulsion Laboratory on March 14, 2004 where many of the myriad of the Genesis entry and planned recovery details were ascertained (kindly provided to lead author by Dr. R. Wiens).

Editorial Handling—Dr. Donald Brownlee

REFERENCES

Anderson J. D. 2000. *Hypersonic and high temperature gas dynamics*. Reston, Virginia: American Institute of Aeronautics and Astronautics. 690 p.

Burnett D. March 14, 2004. Genesis science team meeting, mission status: PowerPoint Presentation (Mission status1.ppt). Pasadena California: NASA Jet Propulsion Laboratory. 47 p.

Cates J. E. and Sturtevant B. 2002. Seismic detection of sonic booms. *Journal of the Acoustical Society of America* 111:614–628.

Edwards W. N., Brown P. G., and ReVelle D. O. Forthcoming. Total bolide yield using measured infrasonic signal properties. *Earth, Moon, and Planets*.

Garrick I. E. and Maglieri D. J. 1968. A summary of results on sonic-boom pressure signature variations associated with atmospheric conditions. NASA Technical Note D-4588. Washington, D.C.: U.S. Government Printing Office.

Hayes W. D., Haefeli R. C., And Kulsrud H. E. 1969. Sonic boom propagation in a stratified atmosphere, with computer program. Nasa Contractor Report #1299.

Hedin A. E., Fleming E. L., Manson A. H., Schmidlin F. J., Avery S. K., Clark R. R., Franke S. J., Fraser G. J., Tsuda T., Vial F., and Vincent R. A. 1996. Empirical wind model for the upper, middle, and lower atmosphere. J*ournal of Atmospheric and Terrestrial Physics* 58:1421–1447.

Henderson H. R. and Hilton D. A. 1974a. Sonic-boom ground-pressure measurements from from the launch and reentry of Apollo 16. NASA Technical Note D-7606. Washington, D.C.: U.S. Government Printing Office.

Henderson H. R. and Hilton D. A. 1974b. Sonic-boom measurements in the focus region during the ascent of Apollo 17. NASA Technical Note D-7806. Washington, D.C.: U.S. Government Printing Office.

Hilton D. A., Henderson H. R., and McKinney R. 1972. Sonic-boom ground-pressure measurements from Apollo 15. NASA Technical Note D-6950. Washington, D.C.: U.S. Government Printing Office.

Hubbard H. H., Maglieri D. J., Huckel V., and Hilton D. A. 1964. Ground measurements of sonic-boom pressures for the altitude range of 10,000 to 75,000 feet. NASA Technical Report R-198. Washington, D.C.: U.S. Government Printing Office.

Kanamori H., Mori J., Sturtevant B., Anderson D. L., and Heaton T. 1992. Seismic excitation by space shuttles. *Shock Waves* 2:89–96.

Picone J. M., Hedin A. E., Drob D. P., and Aikin A. C. 2002. NRLMSISE-00 empirical model of the atmosphere: Statistical comparisons and scientific issues. *Journal of Geophysical Research* 107:1468, doi:10.1029/2002JA009430,2002.

Plooster M. N. Shock waves from line sources. 1968. NCAR Technical Note #37. Boulder, Colorado: National Center for Atmospheric Research. 84 p.

Plooster M. N. 1971. Numerical simulations of spark discharges in air. *Physics of Fluids* 14:2111–2123.

ReVelle D. O., Mutschlecner J. P., Sandoval T. D., Brown P. G., and Whitaker R. W. 2003. Interim final LANL report: Los Alamos infrasonic signals from the reentry and break-up of the shuttle Columbia. 46 p.

Revelle D. O., Brown P. G., and Spurny P. 2004. Entry dynamics and acoustics/infrasonic/seismic analysis for the Neuschwanstein meteorite fall. *Meteoritics & Planetary Science* 39:1605–1626.

ReVelle D. O. 2001. Theoretical Leonid modeling. Proceedings, Meteoroids Conference. pp. 149–157.

ReVelle D. O. 2002. Fireball dynamics, energetics, ablation, luminosity, and fragmentation modeling. Proceedings, Asteroids, Comets, Meteors Conference. pp. 127–136.

ReVelle D. O. Forthcoming. Recent advances in bolide modeling: A bolide potpourri. *Earth, Moon, and Planets*.

Whitham G. B. 1950. The behavior of supersonic flow past a body of revolution far from the axis. *Proceedings of the Royal Society of London A* 201:89–109.